iScience, Volume *25*

Supplemental information

The origin of bladder cancer from mucosal field effects

Jolanta Bondaruk, Roman Jaksik, Ziqiao Wang, David Cogdell, Sangkyou Lee, Yujie Chen, Khanh Ngoc Dinh, Tadeusz Majewski, Li Zhang, Shaolong Cao, Feng Tian, Hui Yao, Paweł Kuś, Huiqin Chen, John N. Weinstein, Neema Navai, Colin Dinney, Jianjun Gao, Dan Theodorescu, Christopher Logothetis, Charles C. Guo, Wenyi Wang, David McConkey, Peng Wei, Marek Kimmel, and Bogdan Czerniak

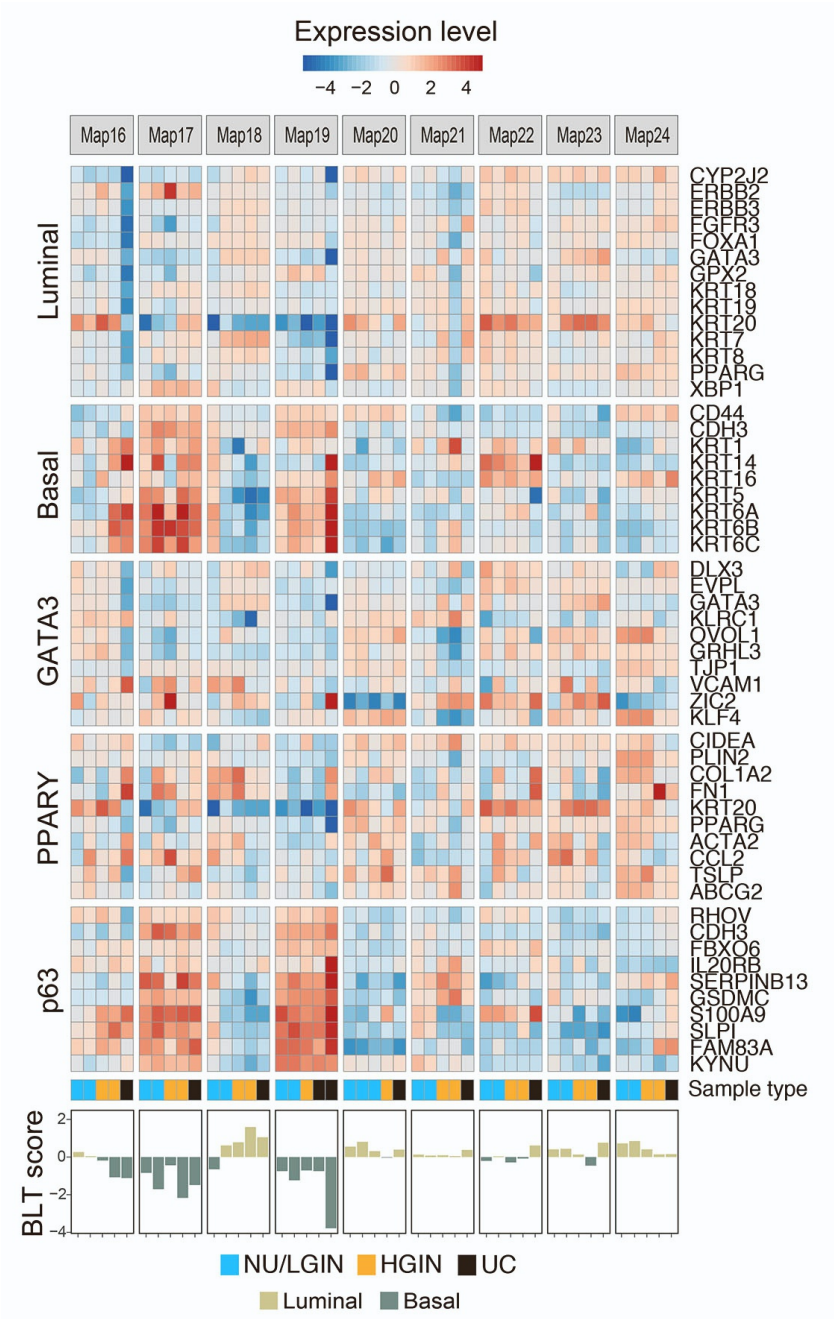

Figure S1. Expression analysis of selected mucosal samples from nine cystectomies corresponding to microscopically normal urothelium (NU), low-grade intraurothelial neoplasia (LGIN), high-grade intraurothelial neoplasia (HGIN), and urothelial carcinoma (UC), related to Figure 1. Gene expression profiling of luminal and basal markers was performed, and it was supplemented by analysis of selected target genes of the luminal transcription factors GATA3 and PPARγ as well as the basal transcription factor p63. Quantitative assessment of the luminal and basal phenotypes was performed using BLT scores. Two cystectomy samples identified as luminal (map 24) and basal (map 19) samples were selected for whole-organ multiplatform genomic profiling.

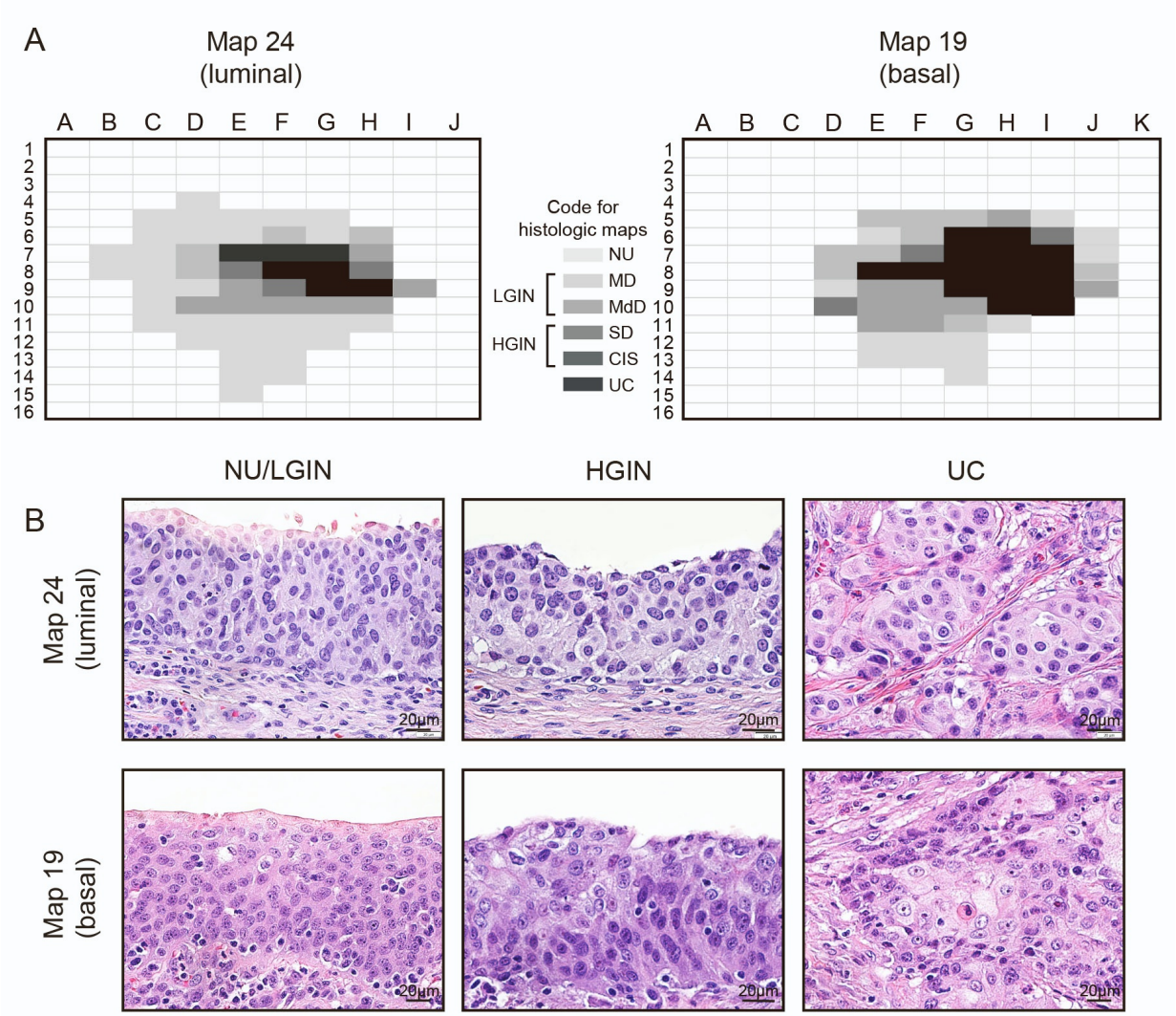

C

	MAP24				MAP19			
	Number of samples				Number of samples			
	All	NU/LGIN	HGIN	UC	All	NU/LGIN	HGIN	UC
RNAseq	40	34	2	4	34	28	4	2
Methylation	36	29	3	4	36	27	3	6
WES	37	32	2	3	29	25	2	2
CNV	36	29	3	4	36	27	3	6

Figure S2. Preparations of whole-organ histologic maps and the summary of their multi-platform genomic characterization, related to Figure 1. (A) Whole-organ histologic maps prepared by sampling of the entire mucosa and the geographic coordinates of individual mucosal samples selected for multi-platform genomic profiling. **(B)** Representative microscopic images in maps 24 and 19 corresponding to NU/LGIN, HGIN, and UC. **(C)** Summary of multi-platform genomic profiling of individual samples of maps 24 and 19.

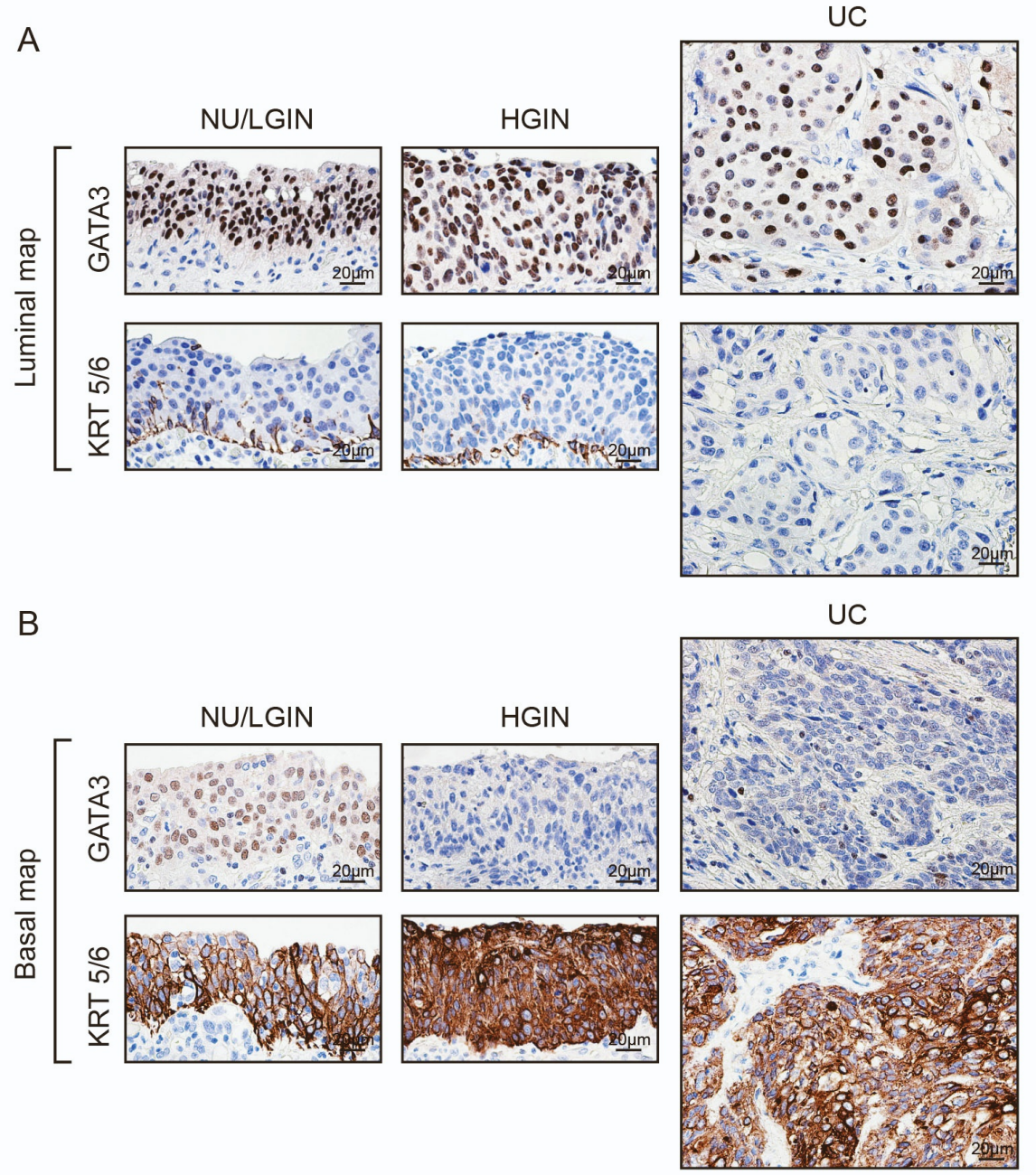

Figure S3. Immunohistochemical analyses of signature luminal (GATA3) and basal (KRT5/6) markers in the progression of neoplasia from mucosal field effects, related to Figure 1. (A) Expression pattern of GATA3 and KRT5/6 in representative samples corresponding to NU/LGIN, HGIN, and UC in the luminal map (map 24). **(B)** Expression pattern of GATA3 and KRT5/6 in representative samples corresponding to NU/LGIN, HGIN, and UC in the basal map (map 19).

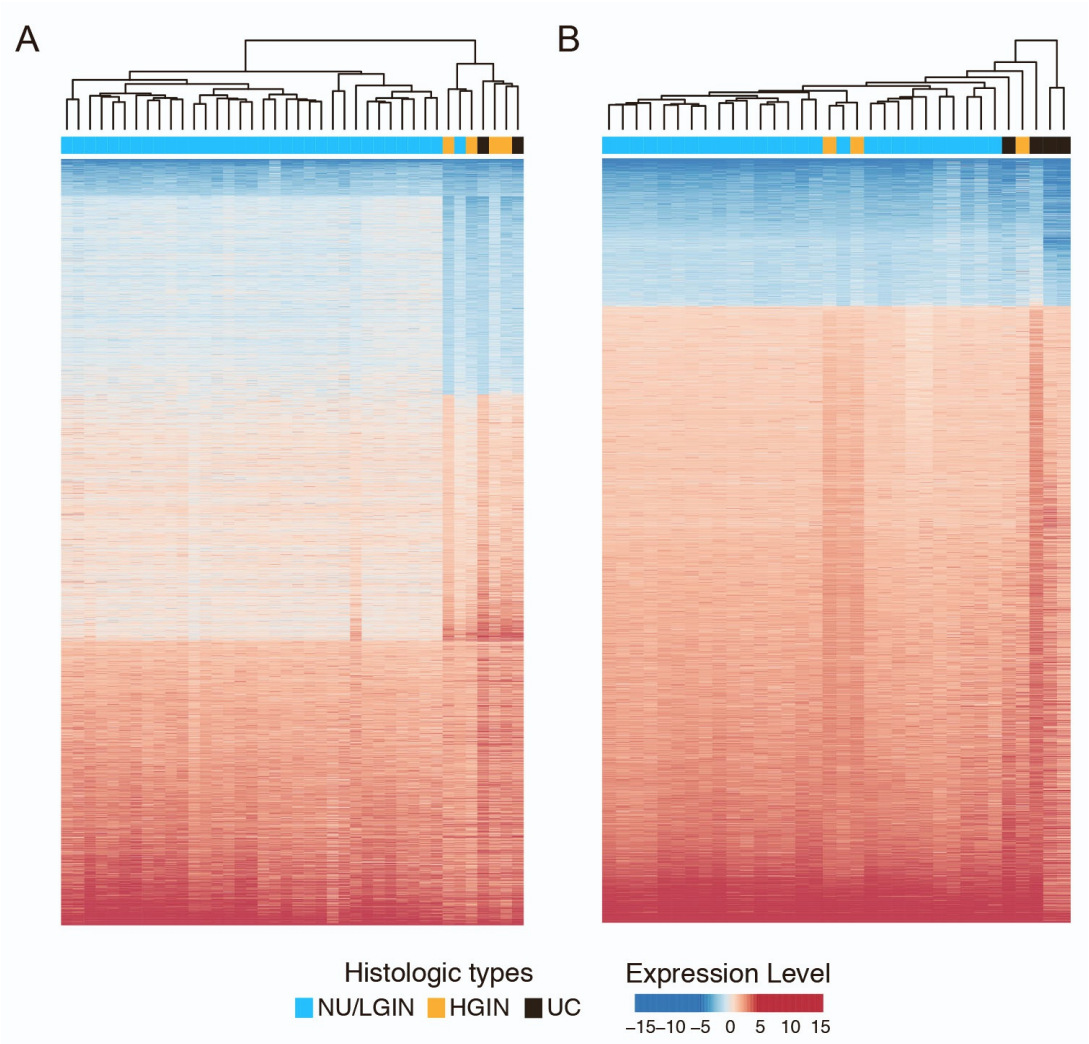

Figure S4. Gene expression changes in evolution of bladder cancer from field effects along the luminal and basal tracks, related to Figure 2. (A) Heat map showing the expression patterns of genes in a cystectomy specimen with luminal cancer (map 24). **(B)** Heat map showing the expression patterns of genes in a cystectomy specimen with basal cancer (map 19).

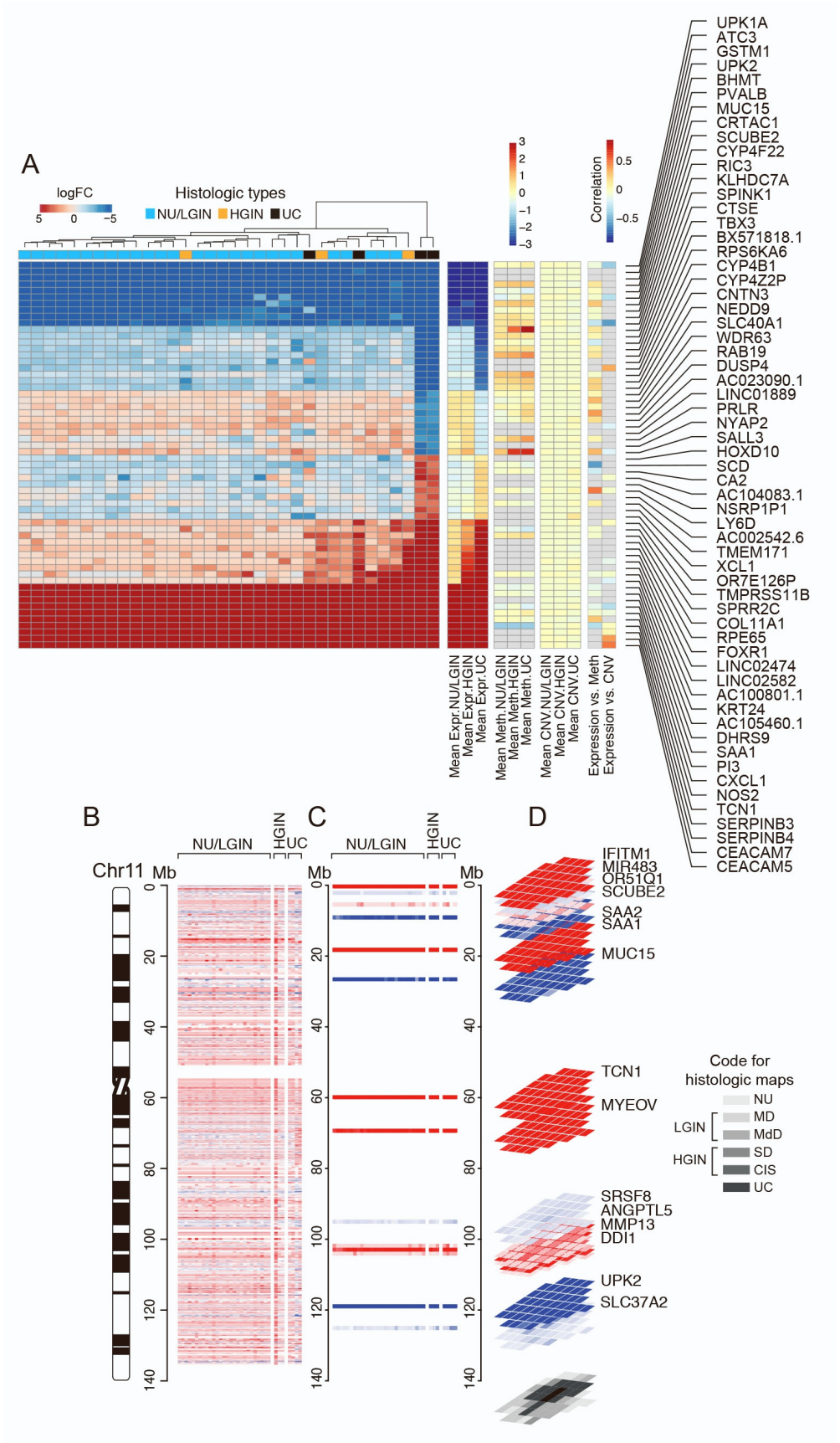
A
logFC
5 0 −5
Histologic types
NU/LGIN HGIN UC
3 2 1 0 −1 −2 −3
Correlation
0.5 0 −0.5
UPK1A
ATC3
GSTM1
UPK2
BHMT
PVALB
MUC15
CRTAC1
SCUBE2
CYP4F22
RIC3
KLHDC7A
SPINK1
CTSE
TBX3
BX571818.1
RPS6KA6
CYP4B1
CYP4Z2P
CNTN3
NEDD9
SLC40A1
WDR63
RAB19
DUSP4
AC023090.1
LINC01889
PRLR
NYAP2
SALL3
HOXD10
SCD
CA2
AC104083.1
NSRP1P1
LY6D
AC002542.6
TMEM171
XCL1
OR7E126P
TMPRSS11B
SPRR2C
COL11A1
RPE65
FOXR1
LINC02474
LINC02582
AC100801.1
KRT24
AC105460.1
DHRS9
SAA1
PI3
CXCL1
NOS2
TCN1
SERPINB3
SERPINB4
CEACAM7
CEACAM5
Mean Expr.NU/LGIN
Mean Expr.HGIN
Mean Expr.UC
Mean Meth.NU/LGIN
Mean Meth.HGIN
Mean Meth.UC
Mean CNV.NU/LGIN
Mean CNV.HGIN
Mean CNV.UC
Expression vs. Meth
Expression vs. CNV
B
NU/LGIN
HGIN
UC
Chr11
Mb
0 20 40 60 80 100 120 140
C
NU/LGIN
HGIN
UC
Mb
0 20 40 60 80 100 120 140
D
IFITM1
MIR483
OR51Q1
SCUBE2
SAA2
SAA1
MUC15
TCN1
MYEOV
SRSF8
ANGPTL5
MMP13
DDI1
UPK2
SLC37A2
Code for histologic maps
NU
MD
MdD
SD
CIS
UC
LGIN
HGIN

Figure S5. Evolution of expression changes from field effects through HGIN to UC in cancer developing along the basal track in map 19, related to Figure 2. (A) Hierarchical clustering of the 60 most downregulated and overexpressed genes showing monotonic expression changes in samples of NU/LGIN through HGIN to UC, HGIN and UC, and UC only. **(B)** Whole-organ expression map for chromosome 11 showing a chromosomal diagram and the expression pattern for genes in individual samples from a cystectomy specimen classified as NU/LGIN, HGIN, and UC. **(C)** Expression pattern for downregulated and overexpressed genes with monotonic changes in NU/LGIN, HGIN, and UC. **(D)** 3D pattern of downregulated and overexpressed genes in the whole-organ map of a cystectomy sample filtered as shown in **C**.

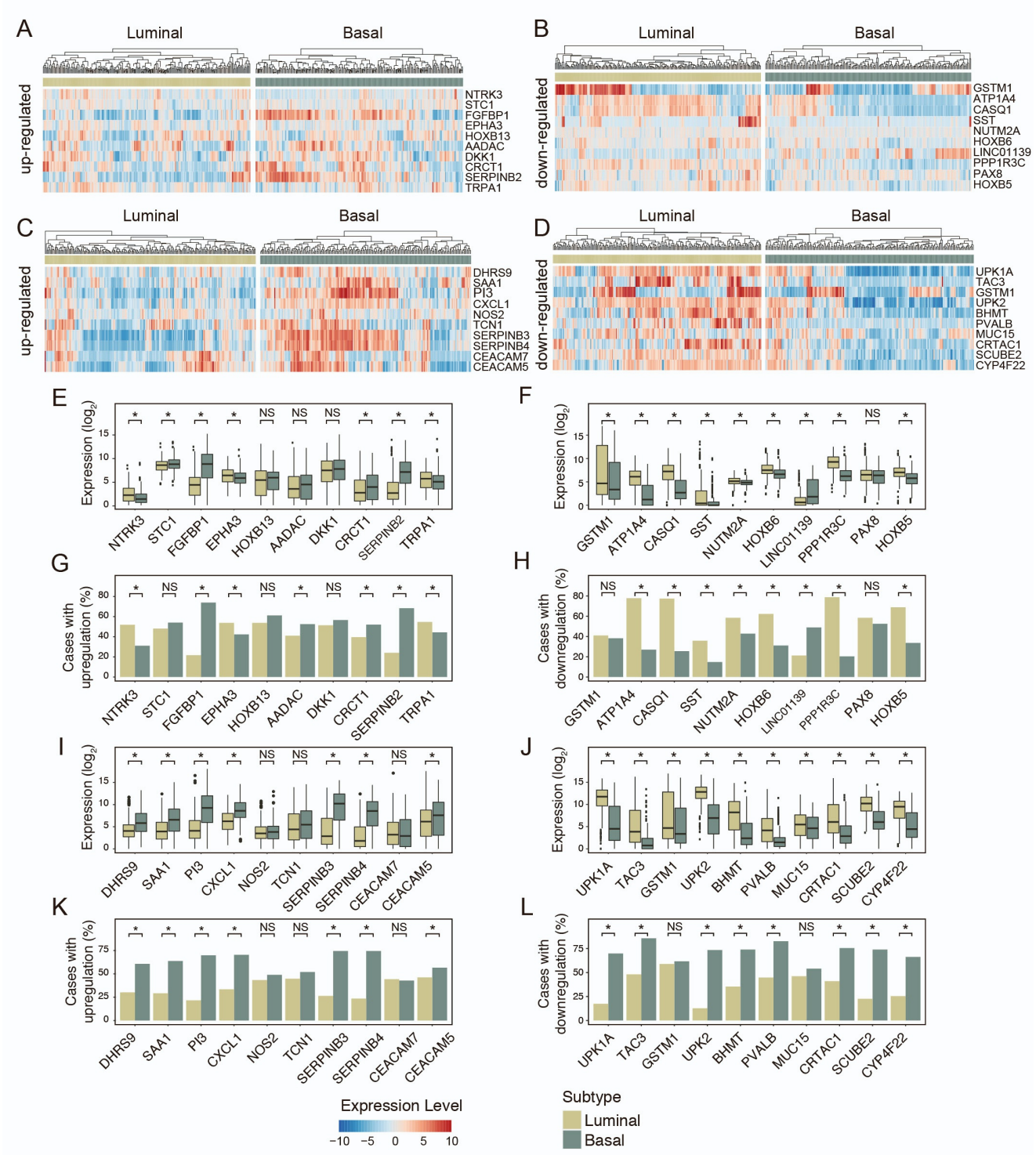
A
Luminal
Basal
up-regulated
NTRK3
STC1
FGFBP1
EPHA3
HOXB13
AADAC
DKK1
CRCT1
SERPINB2
TRPA1
B
Luminal
Basal
down-regulated
GSTM1
ATP1A4
CASQ1
SST
NUTM2A
HOXB6
LINC01139
PPP1R3C
PAX8
HOXB5
C
Luminal
Basal
up-regulated
DHRS9
SAA1
PI3
CXCL1
NOS2
TCN1
SERPINB3
SERPINB4
CEACAM7
CEACAM5
D
Luminal
Basal
down-regulated
UPK1A
TAC3
GSTM1
UPK2
BHMT
PVALB
MUC15
CRTAC1
SCUBE2
CYP4F22
E
Expression (log2)
F
Expression (log2)
G
Cases with upregulation (%)
H
Cases with downregulation (%)
I
Expression (log2)
J
Expression (log2)
K
Cases with upregulation (%)
L
Cases with downregulation (%)
Expression Level
−10 −5 0 5 10
Subtype
Luminal
Basal

Figure S6. Expression patterns for the 10 most overexpressed and downregulated genes identified in the early field effects and validated in the TCGA cohort, related to Figure 2. (A) Expression pattern for the 10 most upregulated genes identified in the field effects in a luminal map and validated in the TCGA cohort. **(B)** Expression pattern for the 10 most downregulated genes identified in the field effects in a luminal map and validated in the TCGA cohort. **(C)** Expression pattern for the 10 most upregulated genes identified in the field effects in a basal map and validated in the TCGA cohort. **(D)** Expression pattern for the 10 most downregulated genes identified in the field effects in a basal map and validated in the TCGA cohort. **(E)** The box plot analysis of expression levels for the 10 most upregulated genes identified in the field effects in a luminal map and validated in the TCGA cohort. **(F)** The box plot analysis of expression levels for the 10 most downregulated genes identified in the field effects in a luminal map and validated in the TCGA cohort. **(G)** The proportion of luminal and basal bladder cancer cases with upregulation of the 10 most upregulated genes identified in a luminal map and validated in the TCGA cohort. **(H)** The proportion of luminal and basal bladder cancer cases with downregulation of the 10 most downregulated genes identified in a luminal map and validated in the TCGA cohort. **(I)** The box plot analysis of expression levels for the 10 most upregulated genes identified in the field effects in a basal map and validated in the TCGA cohort. **(J)** The box plot analysis of expression levels for the 10 most downregulated genes identified in the field effects in a basal map and validated in the TCGA cohort. **(K)** The proportion of luminal and basal bladder cancer cases with upregulation of the 10 most upregulated genes identified in a basal map and validated in the TCGA cohort. **(L)** The proportion of luminal and basal bladder cancer cases with downregulation of the 10 most downregulated genes in a basal map and validated in the TCGA cohort. Asterisks indicate statistically significant (p value <0.05) difference based on Wilcoxon rank-sum test (Panels E, F, I and J) and chi-squared test (Panels G, H, K and L); NS, not significant difference (p value ≥0.05).

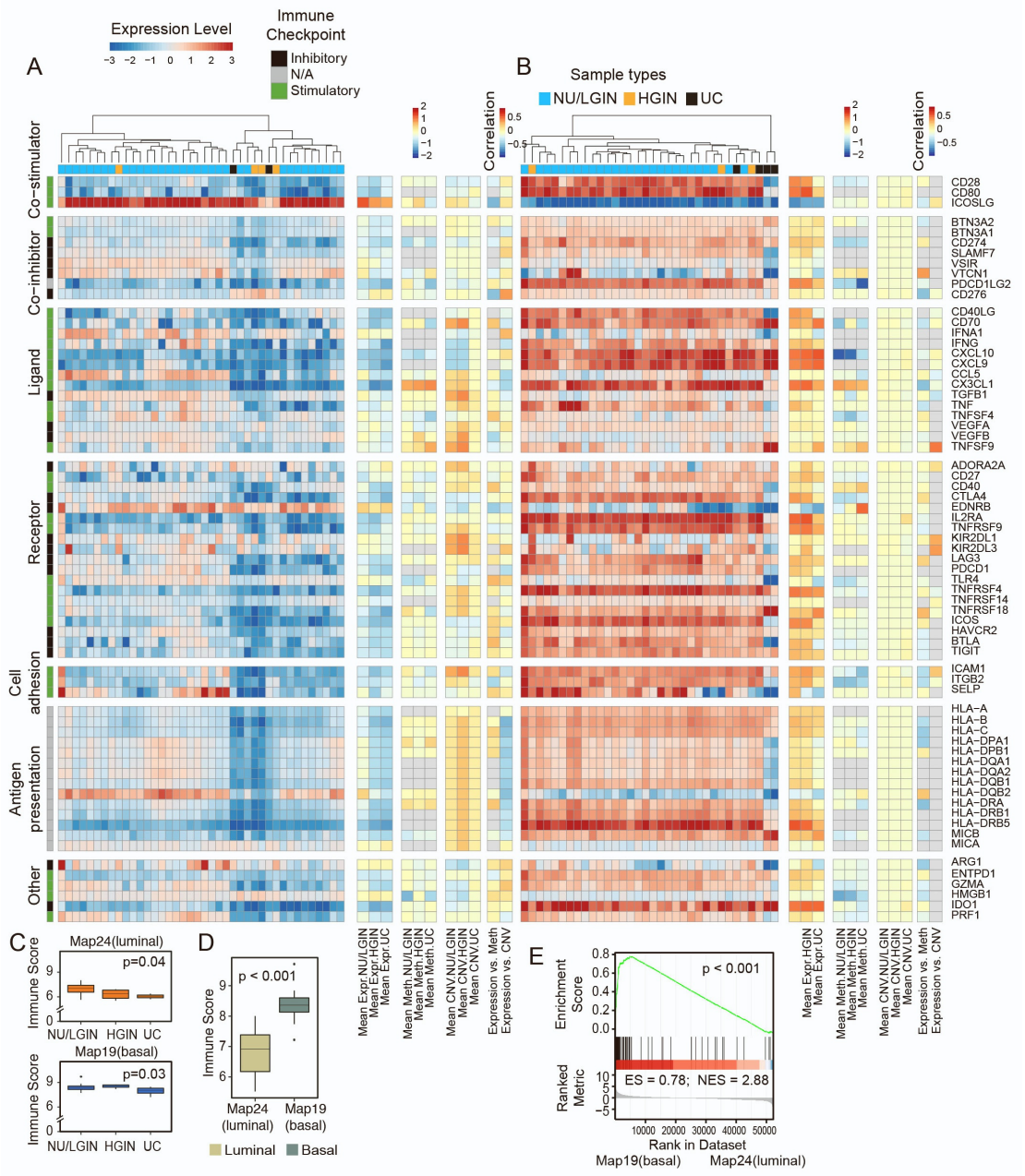

Figure S7. The immune microenvironment based on the expression of immune-regulatory genes in the evolution of bladder cancer along the luminal and basal tracks, related to Figure 4. (A) Expression pattern for immune-regulatory genes in mucosal samples from a cystectomy specimen with luminal cancer. **(B)** Expression pattern for immune-regulatory genes in mucosal samples from a cystectomy specimen with basal cancer. Pearson's correlation coefficients are shown. **(C)** Box plots of immune regulatory genes calculated using their expression profiles in **A** and **B** of map 24 (top) and map 19 (bottom) for subsets of samples classified as NU/LGIN, HGIN, and UC. **(D)** Comparison of immune regulatory gene scores for luminal (map 24) and basal (map 19) cancers. **(E)** GSEA for immune regulatory genes in map 24 (luminal) and map 19 (basal). For (C) and (D) p values were calculated using Kruskal-Wallis test.

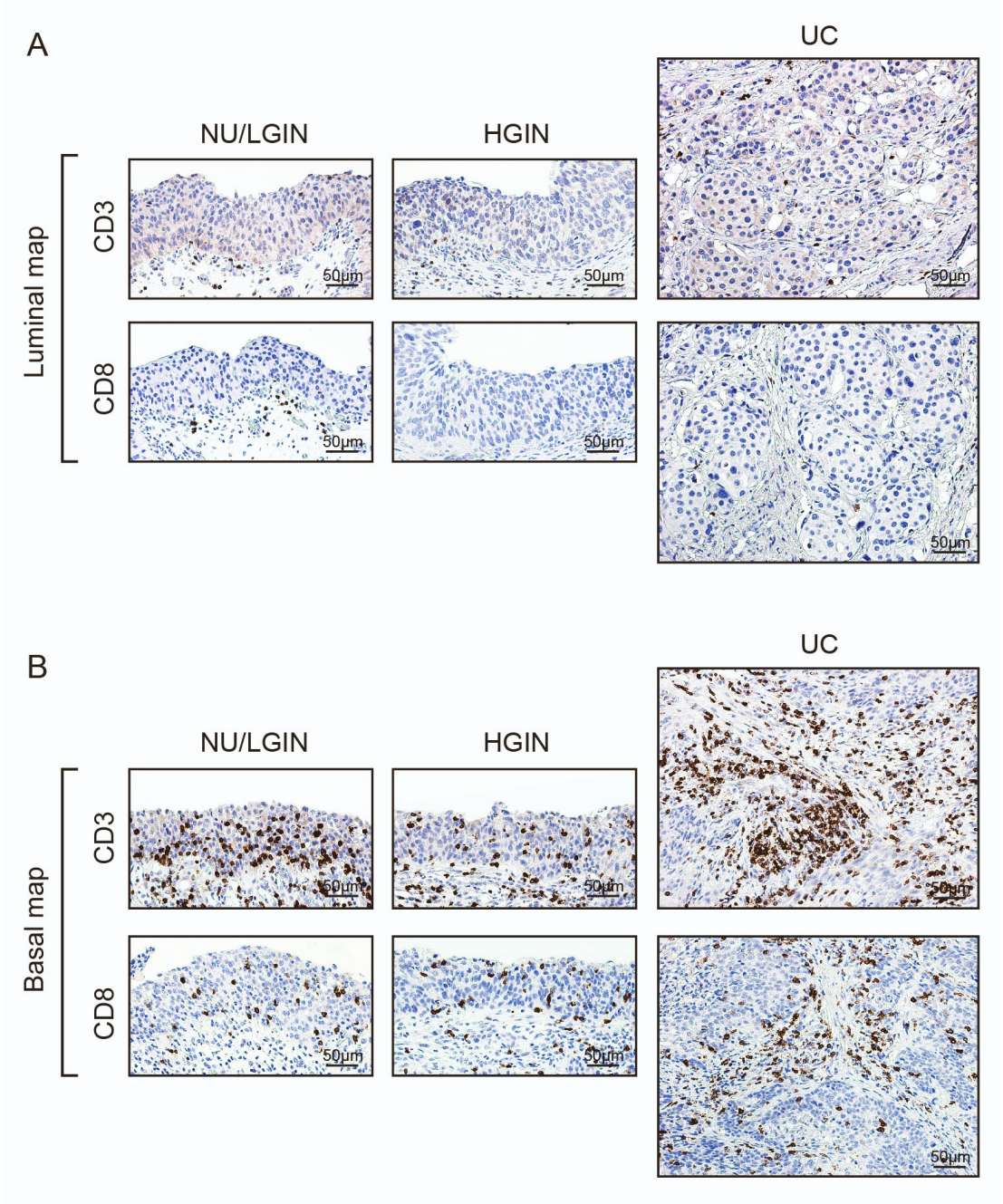

Figure S8. Immunohistochemical expression of CD3 and CD8 T lymphocytes in evolution of neoplasia from mucosal field effects, related to Figure 4. (A) The absence of CD3 and CD8 lymphocytic infiltrates in representative samples of NU/LGIN, HGIN, and UC in the luminal map (map24). **(B)** Brisk lymphocytic CD3 and CD8 lymphocytic infiltrate in representative samples of NU/LGIN, HGIN, and UC in the basal map (map 19).

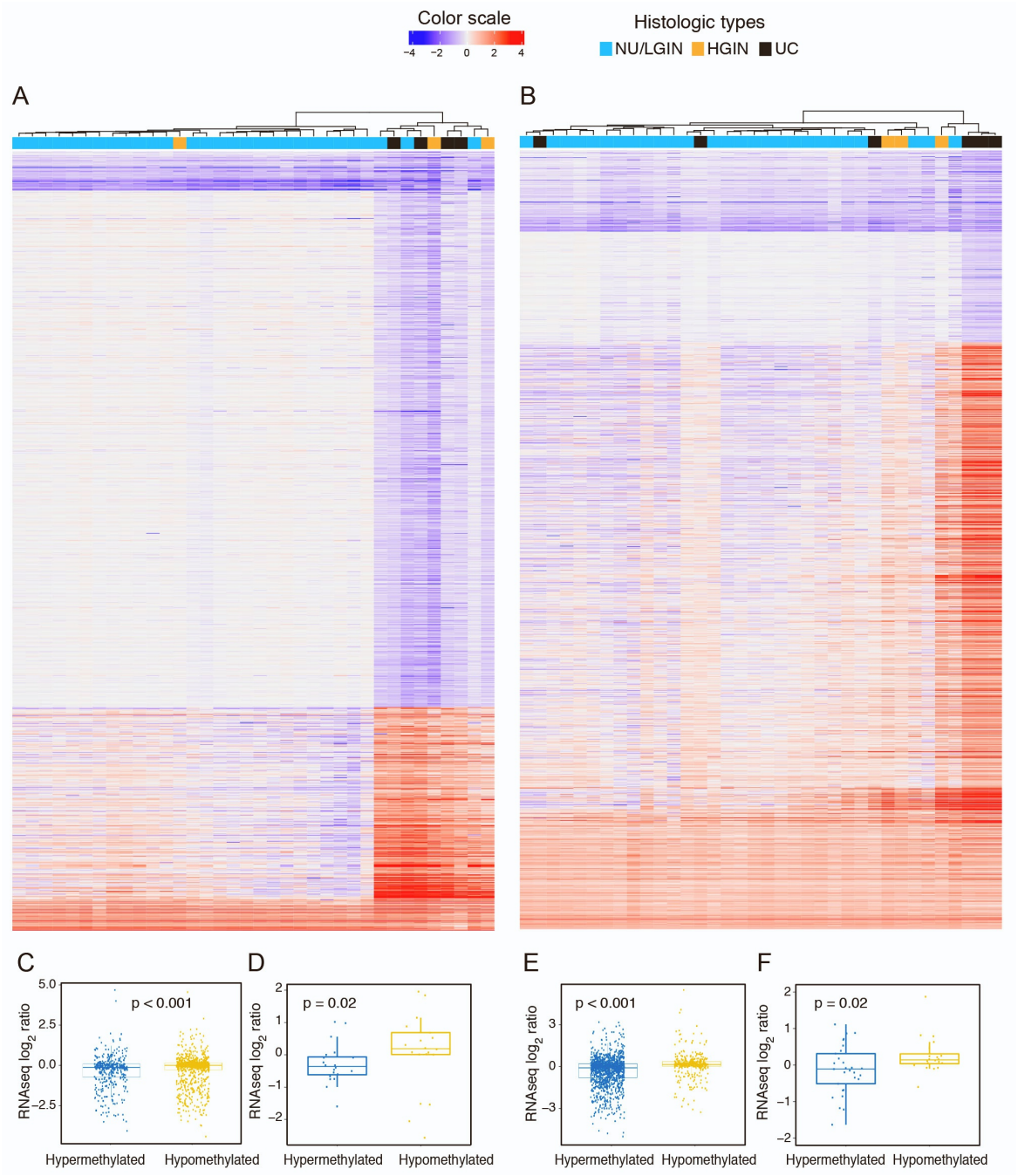

Figure S9. Gene methylation changes in bladder cancer evolving from field effects along the luminal and basal tracks, related to Figure 5. (A) Heat map of the methylation patterns for genes in a cystectomy specimen with luminal cancer in map 24. **(B)** Heat map of the methylation patterns for genes in a cystectomy specimen with basal cancer in map 19. **(C)** Box plot analysis of the expression levels of hypermethylated and hypomethylated genes in the luminal map (map 24). **(D)** Box plot analysis of top monotonic dysmethylated genes in the luminal map (map 24). **(E)** Box plot analysis of the expression levels of hypermethylated and hypomethylated genes in the basal map (map 19). **(F)** Box plot analysis of top monotonic dysmethylated genes in the basal map (map 19). For (C), (D), (E) and (F) p values were calculated using Wilcoxon test.

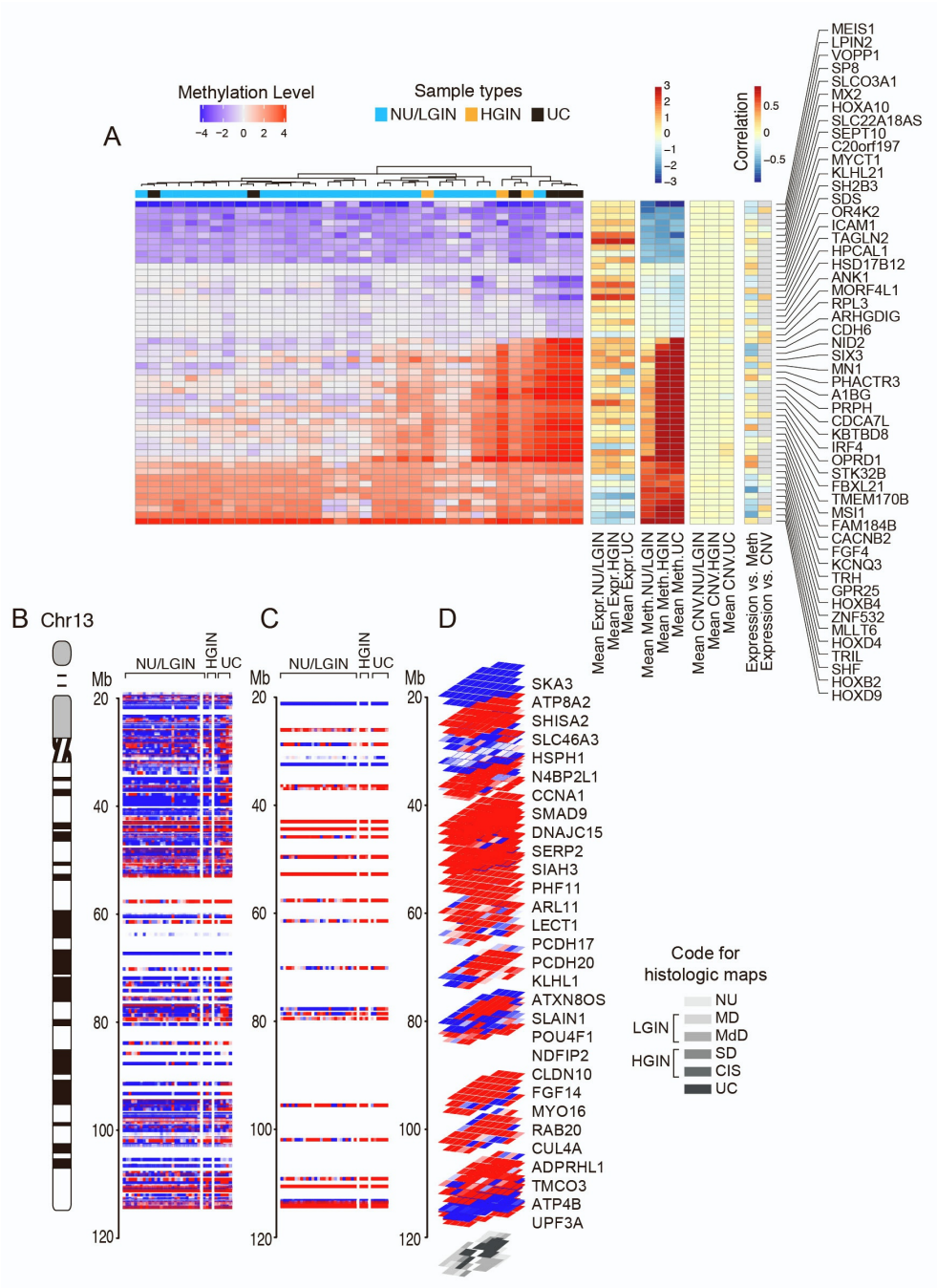

Figure S10. Evolution of methylation changes in development of bladder cancer from field effects through HGIN to UC along the basal track in map 19, related to Figure 5. (A) Hierarchical clustering of the 52 most hypomethylated and hypermethylated genes with monotonic expression changes in samples of NU/LGIN through HGIN to UC, HGIN and UC, and UC only. Pearson's correlation coefficients are shown. **(B)** Whole-organ expression map for chromosome 13 showing a chromosomal diagram and methylation pattern for genes in individual samples from a cystectomy specimen classified as NU/LGIN, HGIN, and UC. **(C)** Methylation pattern for hypomethylated and hypermethylated genes with monotonic methylation changes involving NU/LGIN, HGIN, and UC. **(D)** 3D pattern of hypomethylated and hypermethylated genes as it relates to the whole-organ map of a cystectomy sample filtered as shown in **C**.

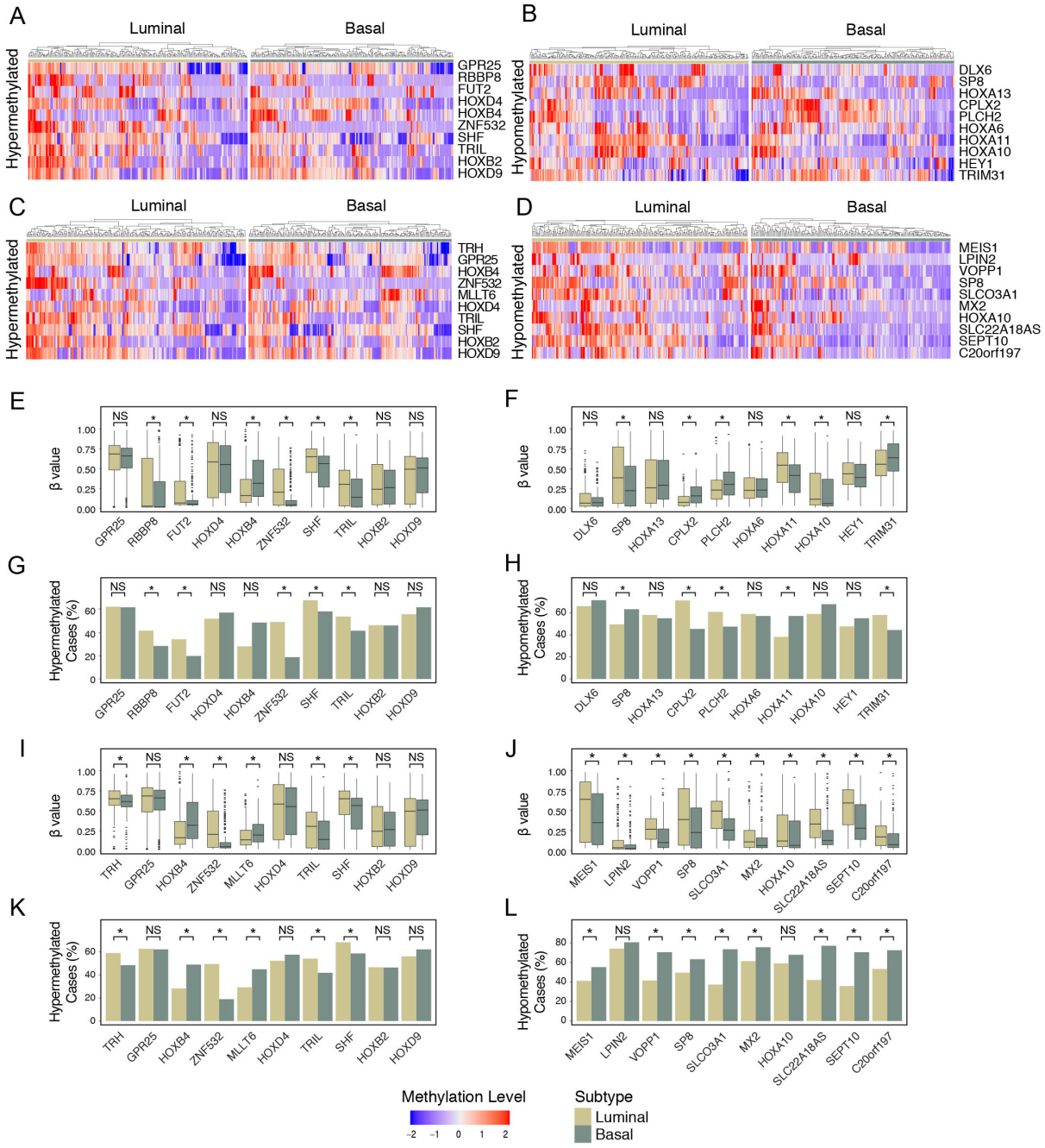
A
Luminal
Basal
Hypermethylated
GPR25
RBBP8
FUT2
HOXD4
HOXB4
ZNF532
SHF
TRIL
HOXB2
HOXD9
B
Luminal
Basal
Hypomethylated
DLX6
SP8
HOXA13
CPLX2
PLCH2
HOXA6
HOXA11
HOXA10
HEY1
TRIM31
C
Luminal
Basal
Hypermethylated
TRH
GPR25
HOXB4
ZNF532
MLLT6
HOXD4
TRIL
SHF
HOXB2
HOXD9
D
Luminal
Basal
Hypomethylated
MEIS1
LPIN2
VOPP1
SP8
SLCO3A1
MX2
HOXA10
SLC22A18AS
SEPT10
C20orf197
E
β value
F
β value
G
Hypermethylated Cases (%)
H
Hypomethylated Cases (%)
I
β value
J
β value
K
Hypermethylated Cases (%)
L
Hypomethylated Cases (%)
NS
*
Methylation Level
−2 −1 0 1 2
Subtype
Luminal
Basal

Figure S11. Methylation patterns for the 10 most hypermethylated and hypomethylated genes identified in the early field effects in the luminal and basal maps and validated in the TCGA cohort, related to Figure 5. (A) Methylation pattern for the 10 most hypermethylated genes identified in the field effects in a luminal map and validated in the TCGA cohort. **(B)** Methylation pattern for the 10 most hypomethylated genes identified in the field effects in a luminal map and validated in the TCGA cohort. **(C)** Methylation pattern for the 10 most hypermethylated genes identified in the field effects in a basal map and validated in the TCGA cohort. **(D)** Methylation pattern for the 10 most hypomethylated genes identified in the field effects in a basal map and validated in the TCGA cohort. **(E)** The box plot analysis of methylation levels for the 10 most hypermethylated genes identified in the field effects in a luminal map and validated in the TCGA cohort. **(F)** The box plot analysis of methylation levels for the 10 most hypomethylated genes identified in the field effects in a luminal map and validated in the TCGA cohort. **(G)** The proportion of luminal and basal bladder cancer cases with hypermethylation of the 10 most hypermethylated genes identified in a luminal map and validated in the TCGA cohort. **(H)** The proportion of luminal and basal bladder cancer cases with hypomethylation of the 10 most hypomethylated genes identified in a luminal map and validated in the TCGA cohort. **(I)** The box analysis of methylation levels for the 10 most hypermethylated genes identified in the field effects in a basal map and validated in the TCGA cohort. **(J)** The box analysis of methylation levels for the 10 most hypomethylated genes identified the field effects in the basal map and validated in the TCGA cohort. **(K)** The proportion of luminal and basal bladder cancer cases with hypermethylation of the 10 most hypermethylated genes identified in a luminal map and validated in the TCGA cohort. **(L)** The proportion of luminal and basal bladder cancer cases with hypomethylation of the 10 most hypomethylated genes identified in a basal map and validated in the TCGA cohort. Asterisks indicate statistically significant (p value <0.05) difference based on Wilcoxon rank sum test (Panels E, F, I, and J) and chi-square test (Panels G, H, K, and L); NS, not significant difference (p value ≥0.05).

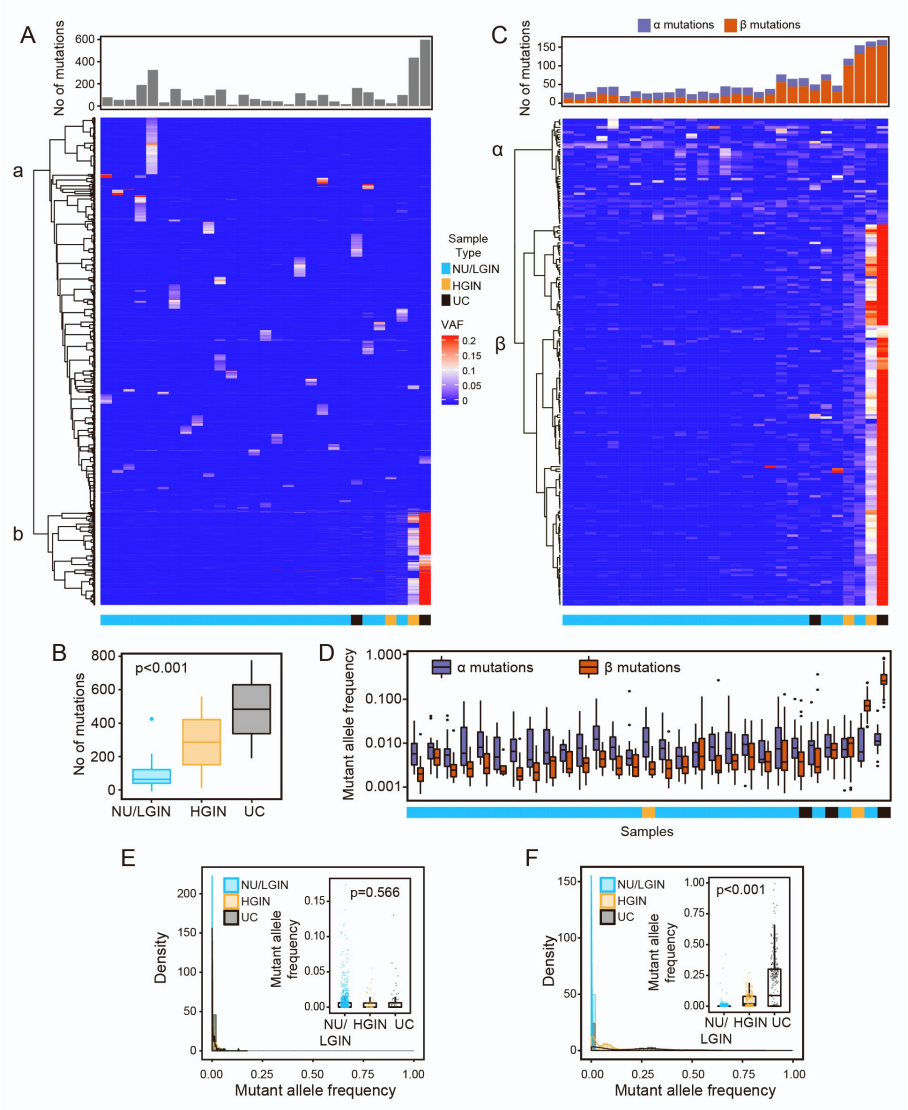

Figure S12. Enrichment of clonal mutations in the evolution of bladder cancer from field effects along the basal track in map 19, related to Figure 6. (A) Heat map of nonsilent mutations showing their VAFs in individual mucosal samples. Number of mutations in individual mucosal samples are shown in the top diagram. **(B)** Box plot analysis of mutations in mucosal samples classified as NU/LGIN, HGIN, and UC. **(C)** Heat map of VAFs (≥0.01) in 198 genes showing variant alleles in at least three mucosal samples. Number of α and β mutations in individual samples is shown in the top diagram. **(D)** Mutant allele frequencies of α and β mutations in individual mucosal samples. **(E)** Density plot showing the clonality of nonsilent VAFs in cluster α with a similar low level of frequency, which decreased in frequency with progression from NU/LGIN to HGIN and UC. Inset, boxplot of VAFs in three groups of mucosal samples of NU/LGIN, HGIN, and UC (Kruskal-Wallis test p value). **(F)** Density plot showing the clonality of nonsilent VAFs in cluster β with a statistically significant increase in clonality with progression from NU/LGIN, HGIN and UC. Inset, boxplot of VAFs in three groups of mucosal samples of NU/LGIN, HGIN, and UC (Kruskal-Wallis test p value). For (B) p values was calculated using ANOVA test.

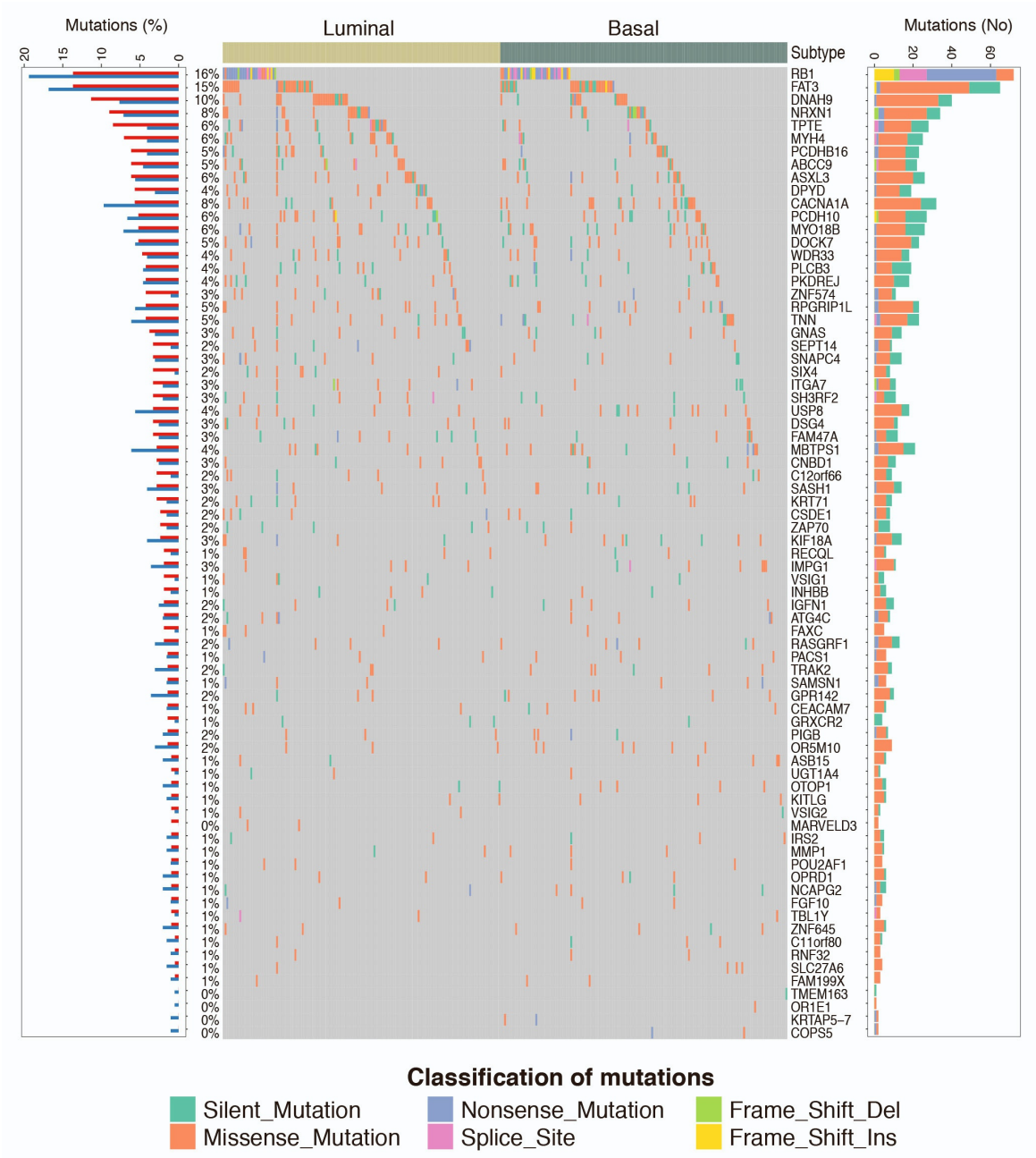

Figure S13. Mutational landscape of 80 mutations with VAFs (≥0.01) showing mutations in at least three samples in a whole-organ luminal map analyzed in the TCGA cohort, related to Figure 6. Mutations of these 80 genes in cluster α were identified in a whole-organ luminal map and shown in cluster α in **Figure 6B** and were analyzed in the TCGA cohort. The bars on the right show the numbers of specific substitutions for individual genes. The bars on the left show the frequencies of mutations in luminal and basal bladder cancers.

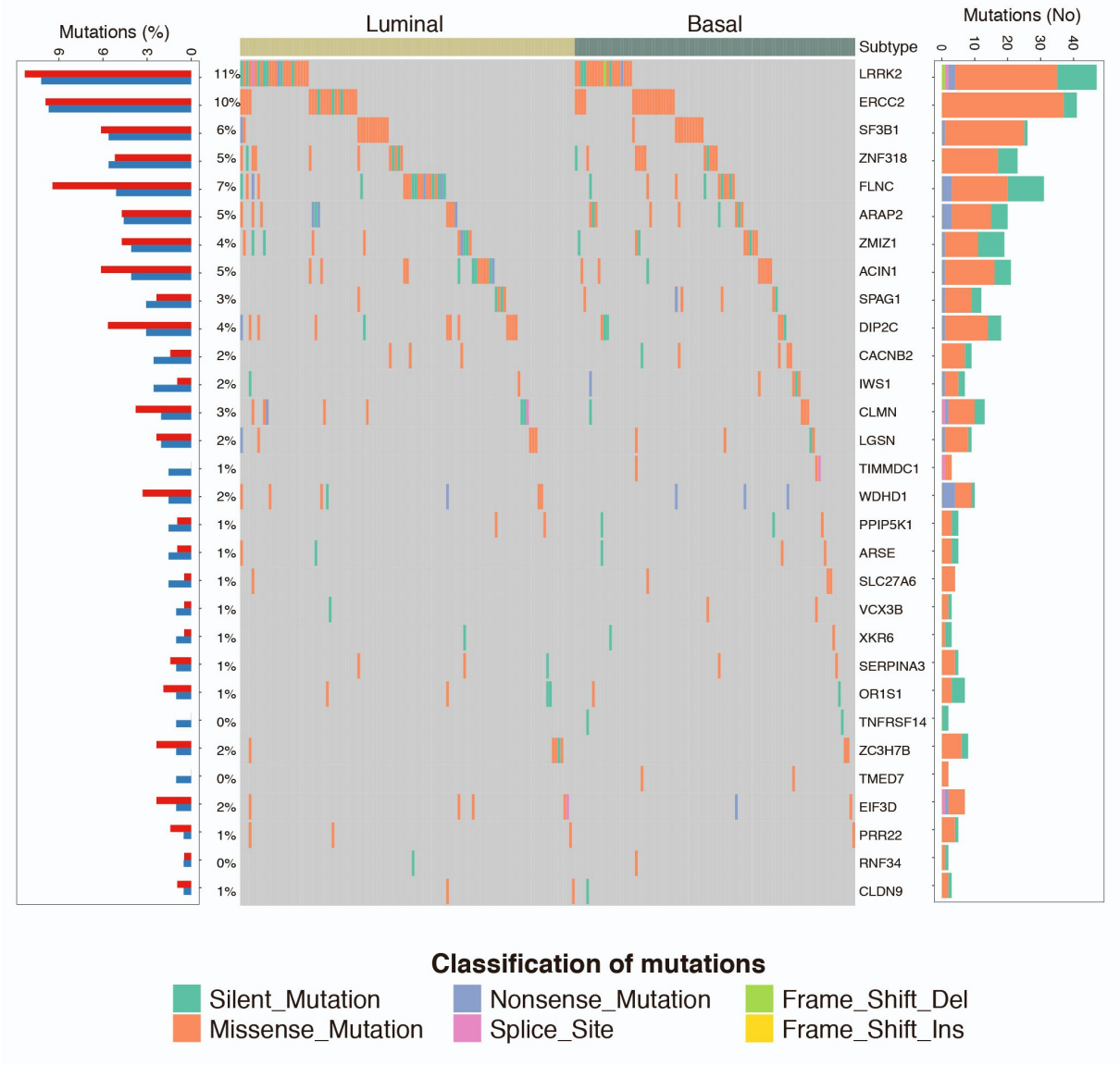

Figure S14. Mutational landscape of 43 mutations with VAFs (≥0.01) showing mutations in at least three samples in a whole-organ basal map analyzed in the TCGA cohort, related to Figure 6. Mutations of these 43 genes in cluster α were identified in a whole-organ basal map and shown in cluster α in **Figure S12B** and were analyzed in the TCGA cohort. The bars on the right show the numbers of specific substitutions for individual genes. The bars on the left show the frequencies of mutations in luminal and basal bladder cancers.

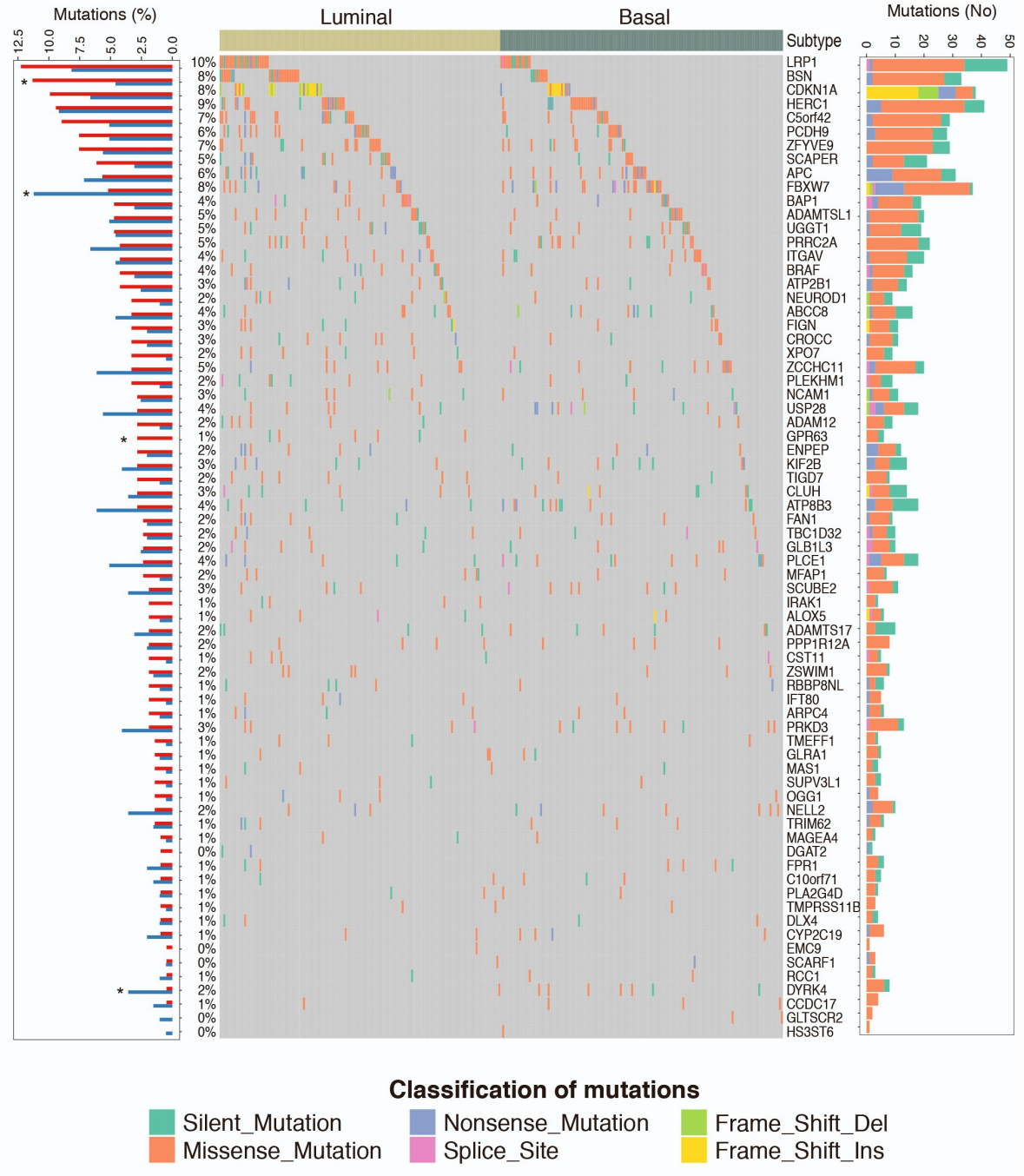

Figure S15. Mutational landscape of 77 mutations with VAFs (≥0.01) showing mutations in at least three samples in a whole-organ luminal map analyzed in the TCGA cohort, related to Figure 6. Mutations of these 77 genes in cluster β were identified in a whole-organ luminal map and shown in cluster β in **Figure 6B** and were analyzed in the TCGA cohort. The bars on the right show the numbers of specific substitutions for individual genes. The bars on the left show the frequencies of mutations in luminal and basal bladder cancers. Asterisks denote genes with significant p-values (<0.05) based on Fisher's exact test.

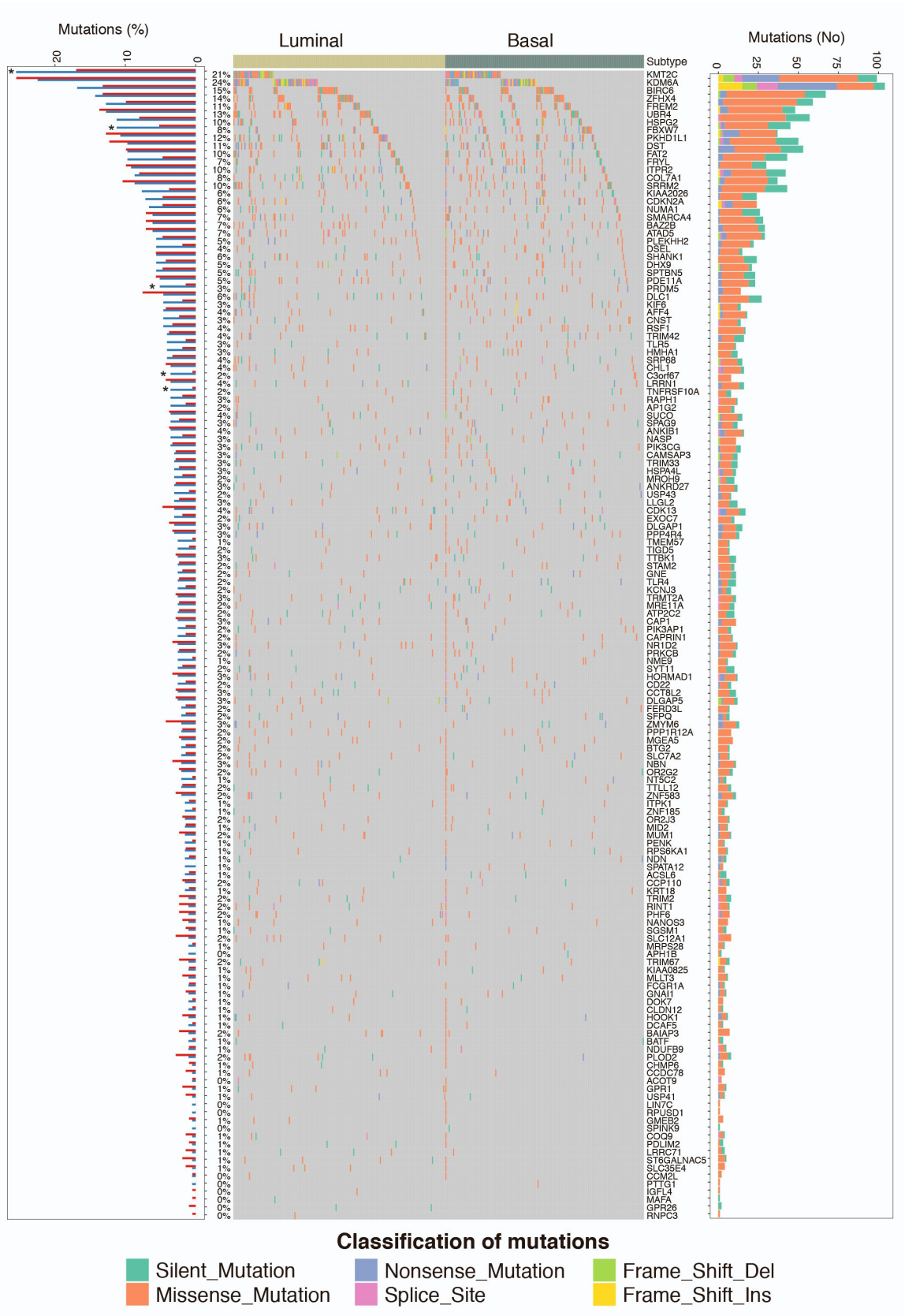
Mutations (%)
Luminal
Basal
Subtype
Mutations (No)
Classification of mutations
Silent_Mutation
Missense_Mutation
Nonsense_Mutation
Splice_Site
Frame_Shift_Del
Frame_Shift_Ins

Figure S16. Mutational landscape of 155 mutations with VAFs (≥0.01) showing mutations in at least three samples in a whole-organ basal map analyzed in the TCGA cohort, related to Figure 6. Mutations of these 155 genes in cluster β were identified in a whole-organ basal map and shown in cluster β in **Figure S12B** and were analyzed in the TCGA cohort. The bars on the right show the number of specific substitutions for individual genes. The bars on the left show the frequency of mutations in luminal and basal bladder cancers. Asterisks denote genes with significant p-values (<0.05) based on Fisher's exact test.

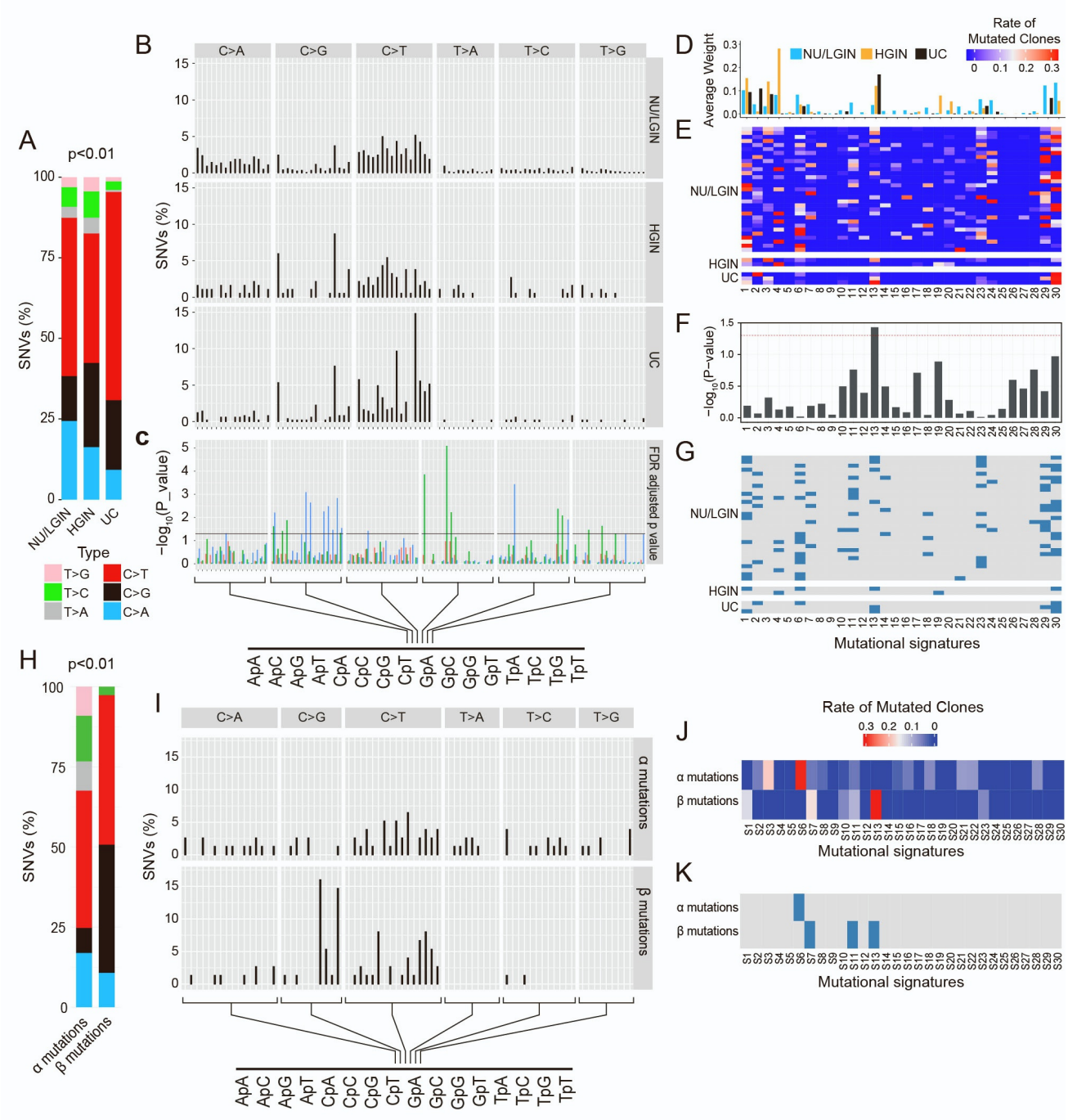
A
p<0.01
SNVs (%)
NU/LGIN
HGIN
UC
Type
T>G
T>C
T>A
C>T
C>G
C>A
B
C>A
C>G
C>T
T>A
T>C
T>G
SNVs (%)
NU/LGIN
HGIN
UC
c
−log10(P_value)
FDR adjusted p value
ApA
ApC
ApG
ApT
CpA
CpC
CpG
CpT
GpA
GpC
GpG
GpT
TpA
TpC
TpG
TpT
D
Average Weight
NU/LGIN
HGIN
UC
Rate of Mutated Clones
E
NU/LGIN
HGIN
UC
F
−log10(P−value)
G
NU/LGIN
HGIN
UC
Mutational signatures
H
p<0.01
SNVs (%)
α mutations
β mutations
I
C>A
C>G
C>T
T>A
T>C
T>G
SNVs (%)
α mutations
β mutations
ApA
ApC
ApG
ApT
CpA
CpC
CpG
CpT
GpA
GpC
GpG
GpT
TpA
TpC
TpG
TpT
J
Rate of Mutated Clones
α mutations
β mutations
Mutational signatures
K
α mutations
β mutations
Mutational signatures

Figure S17. Mutagenesis patterns as they evolve from field effects in bladder cancer developing along the luminal track in map 24, related to Figure 6. (A) Composite bar graphs showing the distribution of all nucleotide substitutions in relation to cancer evolution from NU/LGIN through HGIN to UC. It shows a significant increase in the number of C>T mutations (Fisher's exact test; $p < 0.001$) that parallels the evolution to HGIN and UC. **(B)** Proportion of SNVs in specific nucleotide motifs for each category of substitution in three sets of samples corresponding to NU/LGIN, HGIN, and UC. **(C)** FDRs for specific nucleotide motifs in the progression of neoplasia from NU/LGIN through HGIN to UC. **(D)** Weight scores for mutagenesis patterns in three groups of samples corresponding to NU/LGIN, HGIN, and UC. **(E)** Weight scores for mutagenesis patterns in individual samples of bladder mucosa. **(F)** Significance of mutational patterns in the progression of neoplasia from NU/LGIN through HGIN to UC. **(G)** Significance of contributions for mutagenesis signatures in individual samples after bootstrapping analysis. The blue boxes indicate p values <0.05. **(H)** Composite bar graphs showing the distribution of nucleotide substitutions in α and β mutations. **(I)** Proportion of SNVs in specific nucleotide motifs for each category of substitution for α and β mutations. **(J)** Weight scores for mutagenesis patterns of α and β mutations. **(K)** Significance of contributions for mutagenesis signatures associated with α and β mutations after bootstrapping analyses. The blue boxes indicate p values <0.05. For (A) and (H) p values were calculated using a test of proportions. For (C) and (F) p values were calculated using Wilcoxon test and a Kruskal-Wallis test, respectively.

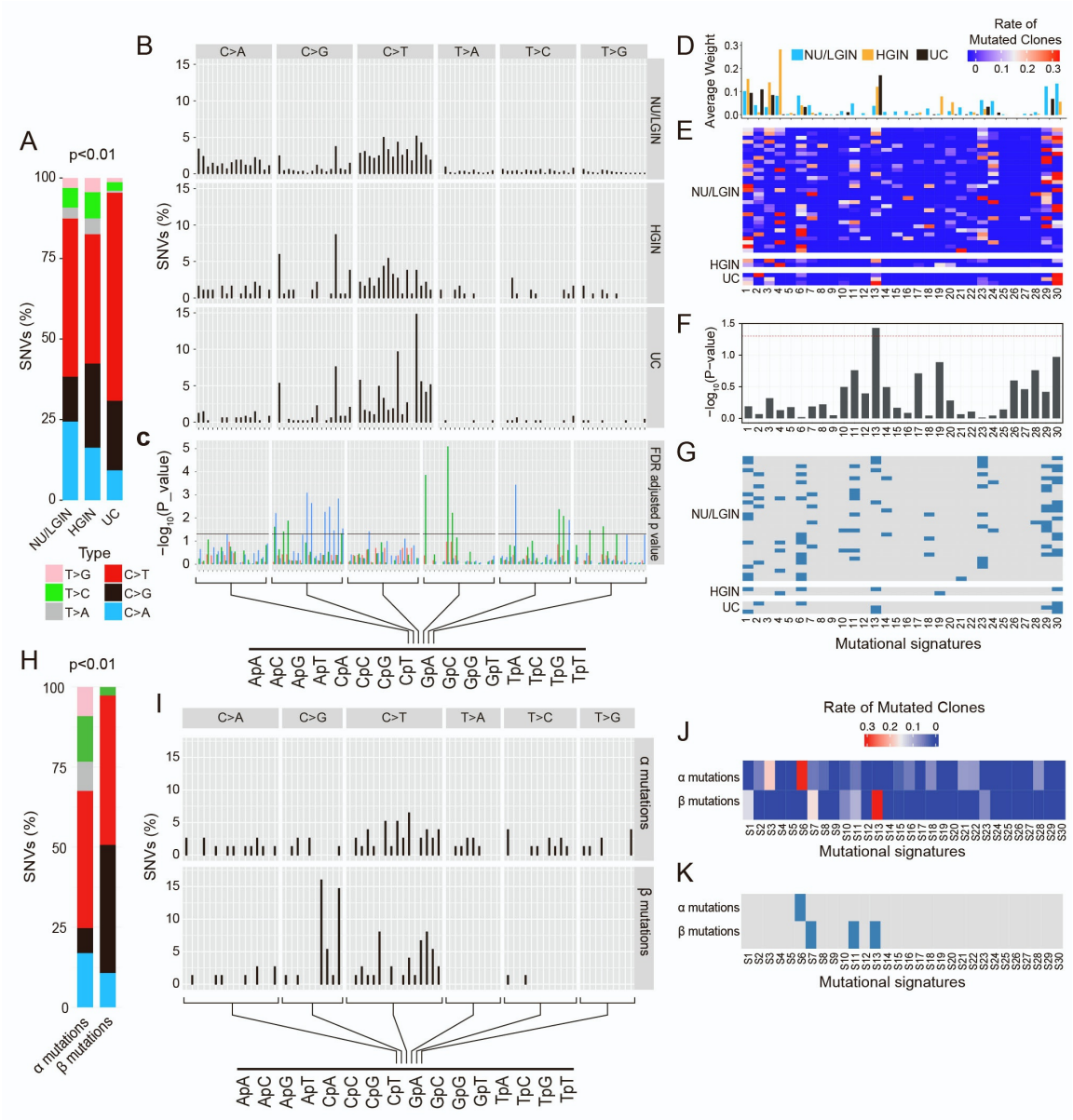
A
p<0.01
SNVs (%)
NU/LGIN
HGIN
UC
Type
T>G
T>C
T>A
C>T
C>G
C>A
B
C>A
C>G
C>T
T>A
T>C
T>G
SNVs (%)
c
−log10(P_value)
FDR adjusted p value
ApA
ApC
ApG
ApT
CpA
CpC
CpG
CpT
GpA
GpC
GpG
GpT
TpA
TpC
TpG
TpT
D
Average Weight
NU/LGIN
HGIN
UC
Rate of Mutated Clones
E
F
−log10(P−value)
G
Mutational signatures
H
p<0.01
α mutations
β mutations
I
J
Rate of Mutated Clones
K
Mutational signatures

Figure S18. Mutagenesis patterns as they evolve from field effects in bladder cancer developing along the basal track in map 19, related to Figure 6. (A) Composite bar graphs showing the distribution of all nucleotide substitutions in relation to cancer evolution from NU/LGIN through HGIN to UC. It shows a significant increase in the number of C>T mutations (Fisher's exact test; $p < 0.001$) that parallels the evolution to HGIN and UC. **(B)** Proportion of SNVs in specific nucleotide motifs for each category of substitution in three sets of samples of NU/LGIN, HGIN, and UC. **(C)** FDRs for specific nucleotide motifs in the progression of neoplasia from NU/LGIN through HGIN to UC. **(D)** Weight scores for mutagenesis patterns in three groups of samples corresponding to NU/LGIN, HGIN, and UC. **(E)** Weight scores for mutagenesis patterns in individual samples of bladder mucosa. **(F)** Significance of mutational patterns in the progression of neoplasia from NU/LGIN through HGIN to UC. **(G)** Significance of contributions of mutagenesis signatures in individual samples after bootstrapping analysis. The blue boxes indicate p values < 0.05. **(H)** Composite bar graphs showing the distribution of nucleotide substitutions in α and β mutations. **(I)** Proportion of SNVs in specific nucleotide motifs for each category of substitution for α and β mutations. **(J)** Weight scores for mutagenesis patterns of α and β mutations. **(K)** Significance of contributions for mutagenesis signatures associated with α and β mutations after bootstrapping analyses. The blue boxes indicate p values <0.05. For (A) and (H) p values were calculated using a test of proportions. For (C) and (F) p values were calculated using Wilcoxon test and a Kruskal-Wallis test, respectively.

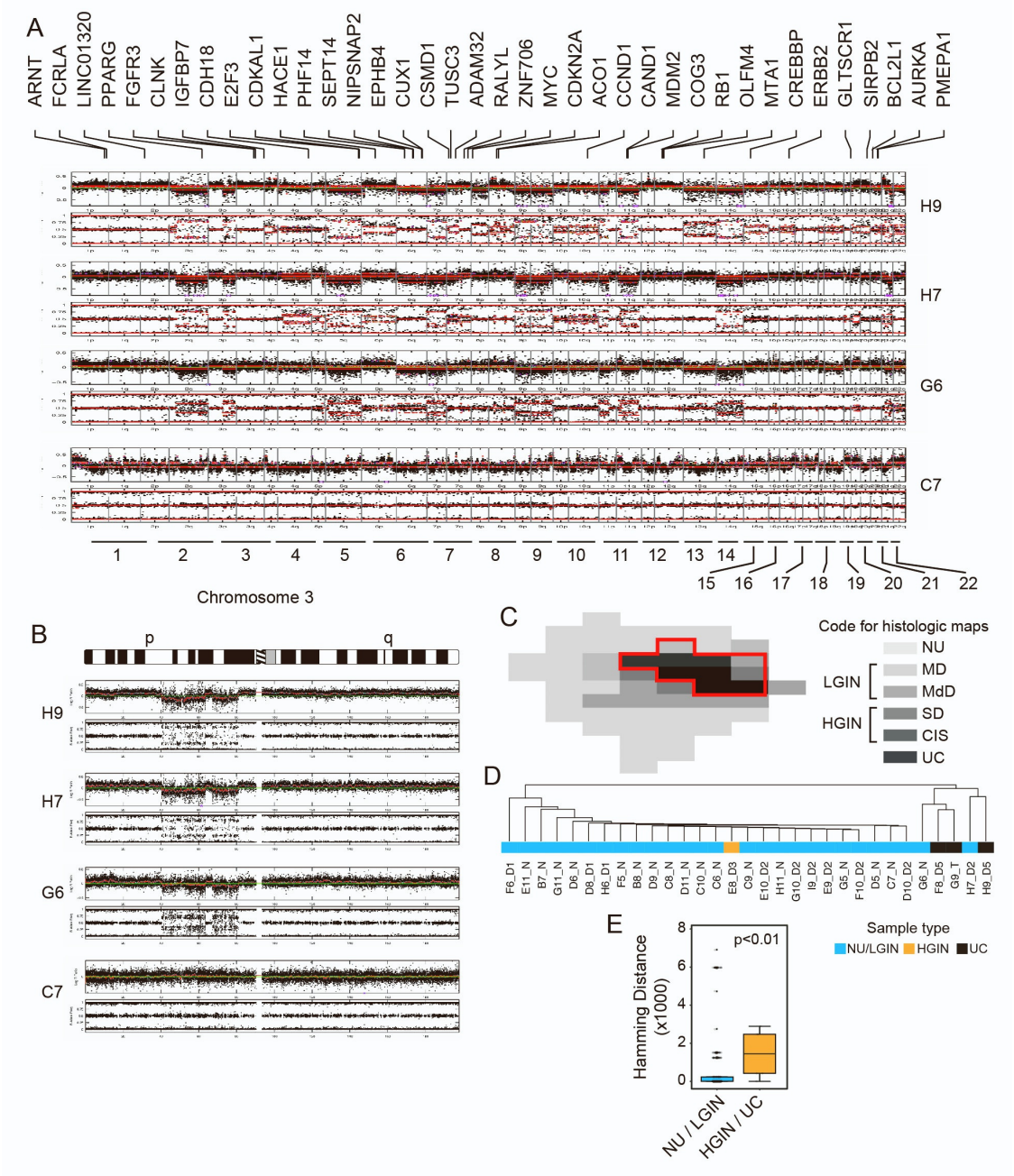

Figure S19. Evolution of copy-number changes from field effects to UC in a luminal map, , related to Figure 7. (A) Log R ratios (top) and B-allele frequencies (bottom) for all chromosomes in representative samples of bladder mucosa reflecting the pattern of progression from NU/LGIN through HGIN to UC. **(B)** Expanded view of chromosome 3 showing log R ratios (top) and B-allele frequencies (bottom) demonstrating segmental loss of chromosome 3p in representative samples of bladder mucosa reflecting the pattern of progression from NU/LGIN through HGIN to UC. **(C)** Histologic map of a luminal cystectomy sample. The red line outlines a plaque of bladder mucosa with widespread genomic changes in CNVs. **(D)** Hierarchical clustering analysis of mucosal samples according to the copy number alterations. **(E)** CNV difference calculated as the Hamming distance in the two groups of samples corresponding to NU/LGIN and HGIN/UC (Wilcoxon rank-sum test p value).

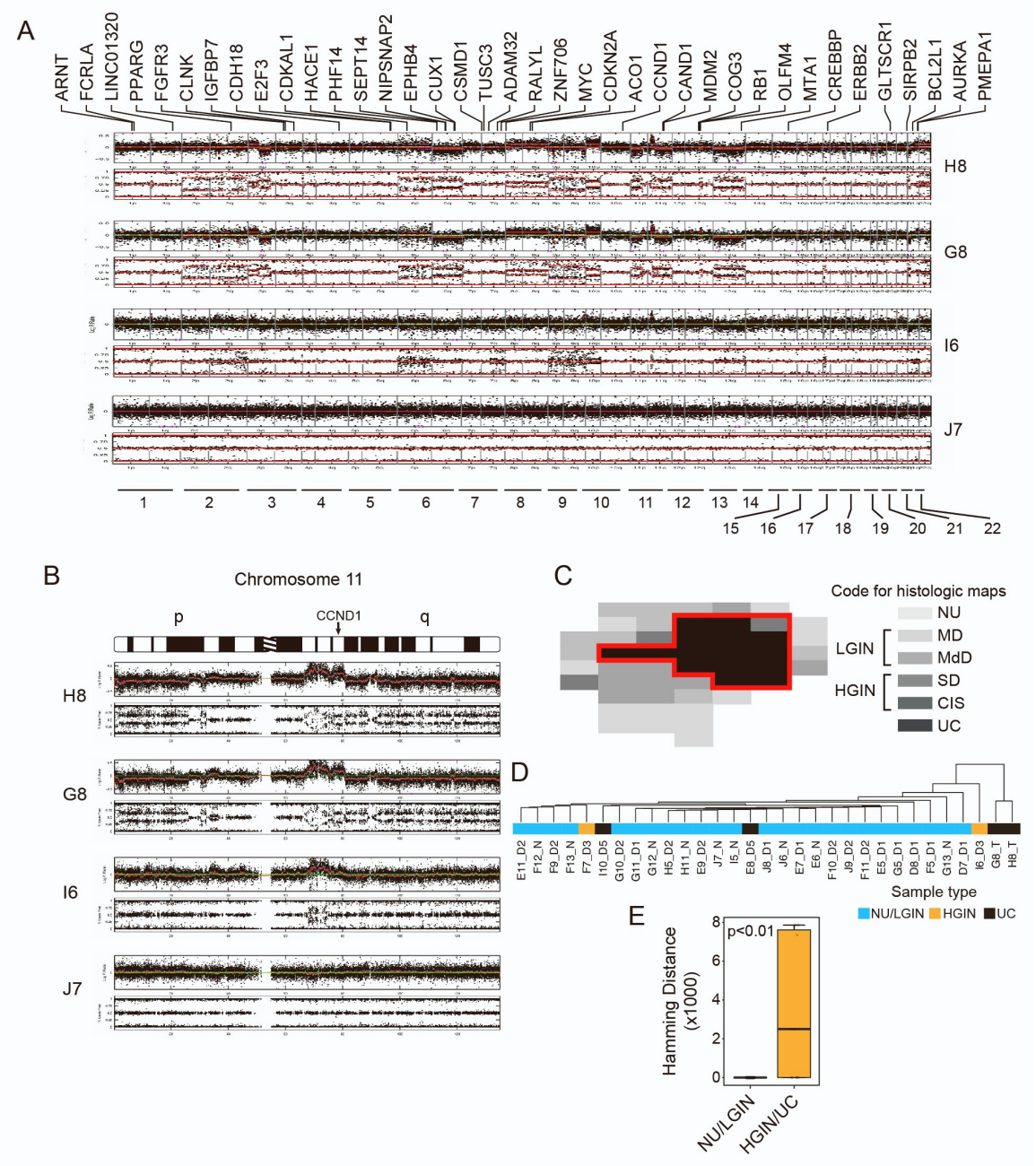

Figure S20. Evolution of copy-number changes from field effects to UC in a basal map, related to Figure 7. (A) Log R ratios (top) and B-allele frequencies (bottom) for all chromosomes in representative samples of bladder mucosa reflecting the pattern of progression from NU/LGIN through HGIN to UC. **(B)** Expanded view of chromosome 11 showing log R ratios (top) and B-allele frequencies (bottom) with segmental amplification chromosome 11q containing CDKD1 in representative samples of bladder mucosa reflecting the pattern of progression from NU/LGIN through HGIN to UC. **(C)** Histologic map of a cystectomy sample. The red line outlines a plaque of bladder mucosa with widespread genomic changes in CNVs. **(D)** Hierarchical clustering analysis of mucosal samples according to the copy number alterations. **(E)** CNV difference calculated as the Hamming distance in the two groups of samples corresponding to NU/LGIN and HGIN/UC (Wilcoxon rank-sum test p value).

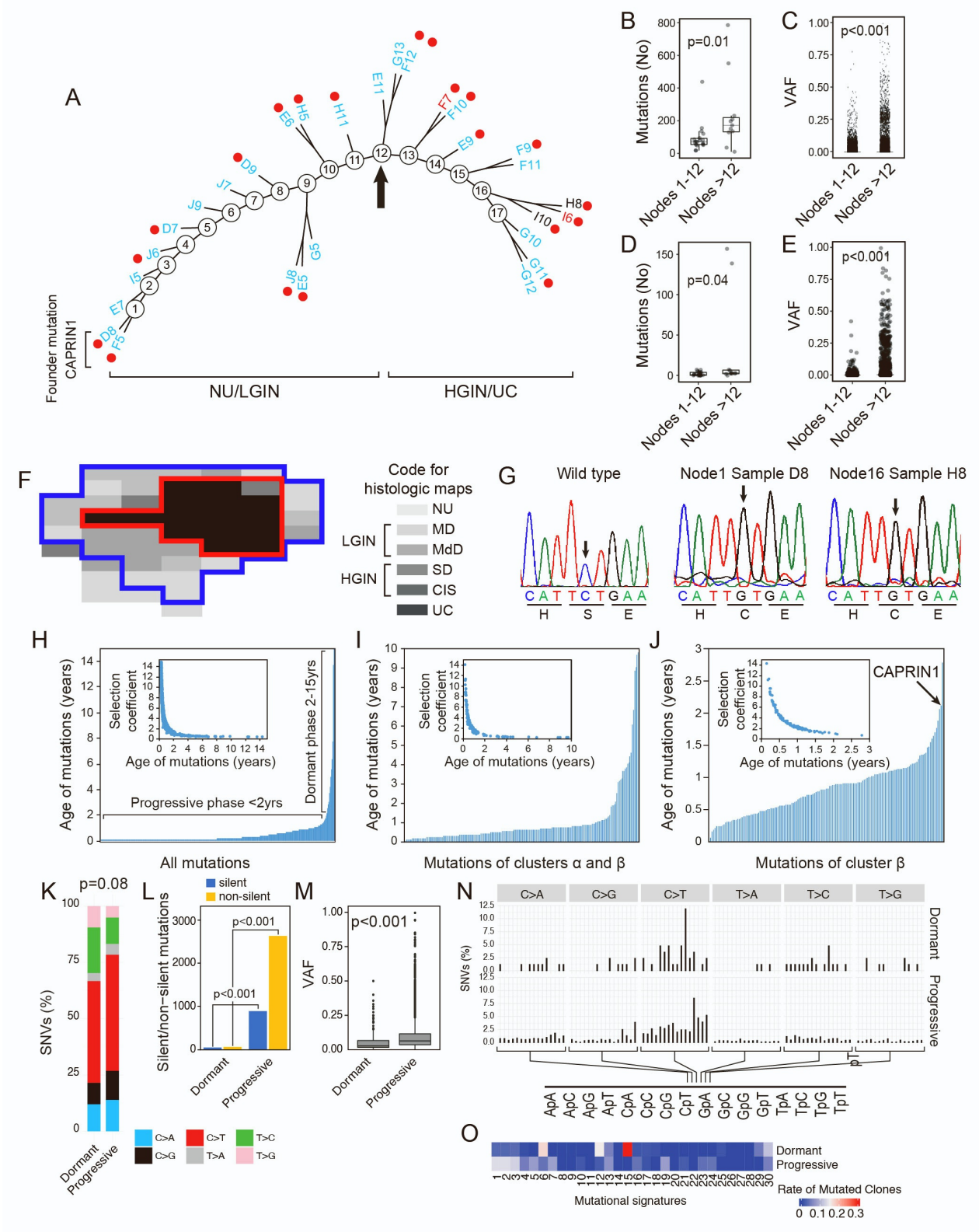
A
Founder mutation
CAPRIN1
NU/LGIN
HGIN/UC
B
Mutations (No)
p=0.01
Nodes 1-12
Nodes >12
C
VAF
p<0.001
D
p=0.04
E
F
Code for histologic maps
NU
MD
MdD
SD
CIS
UC
LGIN
HGIN
G
Wild type
Node1 Sample D8
Node16 Sample H8
H
Age of mutations (years)
Selection coefficient
Progressive phase <2yrs
Dormant phase 2-15yrs
All mutations
I
Mutations of clusters α and β
J
CAPRIN1
Mutations of cluster β
K
p=0.08
SNVs (%)
Dormant
Progressive
L
silent
non-silent
Silent/non-silent mutations
p<0.001
M
VAF
N
C>A
C>G
C>T
T>A
T>C
T>G
O
Mutational signatures
Rate of Mutated Clones

Figure S21. Reconstruction of the evolutionary tree in bladder cancer developing along the basal track in map 19, related to Figure 7. (A) Parsimony analysis showing an evolutionary tree with 17 nodes of expansion of successive clones in the field effects corresponding to NU/LGIN. Node 13 signifies the progression to HGIN, and all samples of HGIN and UC evolved through four additional waves of clonal evolution (nodes 14-17). **(B)** Numbers of all nonsynonymous mutations in mucosal samples of nodes 1-12 and nodes >12. **(C)** VAFs of all nonsynonymous mutations in samples connected to nodes 1-12 and nodes >12 (Wilcoxon rank-sum p value). **(D)** Numbers of mutations in cluster β in nodes 1-12 and nodes >12. **(E)** VAFs of mutations in cluster β in nodes 1-12 and >12 (Wilcoxon rank-sum p value). **(F)** Histologic map of a cystectomy specimen. The blue line outlines a plaque of bladder mucosa with a mutation of a founder gene (*CAPRIN1).* The red line outlines a plaque of bladder mucosa with widespread genomic changes in CNVs. **(G)** Validation of *CAPRIN1* mutational inactivation by Sanger sequencing. Variant allele of *CAPRIN1* DNA tracings are shown in selected mucosal samples and compared to the wild-type sequence **(H)** Mathematical modeling of bladder cancer evolution from field effects using all nonsynonymous mutations. Inset, the selection coefficient related to the ages of the mutations. **(I)** Mathematical modeling of bladder cancer evolution from field effects using clonally expanding mutations in clusters α and β. Inset, the selection coefficient related to the ages of the mutations. **(J)** Mathematical modeling of bladder cancer evolution from field effects using clonally expanding mutations in cluster β. Inset, the selection coefficient related to the ages of the mutations. Wilcoxon rank-sum test p values in panels B, C, D, and E. **(K)** Composite bar graph showing the distribution of all nucleotide substitutions in dormant and progressive phases of bladder cancer development. **(L)** Bar plots showing the number of silent and non-silent mutations in the dormant and progressive phases of bladder cancer development. **(M)** VAF in dormant and progressive phases of bladder cancer development. **(N)** Proportion of SNVs in specific nucleotide motifs for each category of substitutions in dormant and progressive phases of bladder cancer development. **(O)** Weight scores for mutagenesis patterns in dormant and progressive phases of bladder cancer development. For (B) and (D) p values were calculated using a Kruskal-Wallis test. For (K) and (L) p values were calculated using a test of proportions. For (M) p values were calculated using a two sample Wilcoxon test.

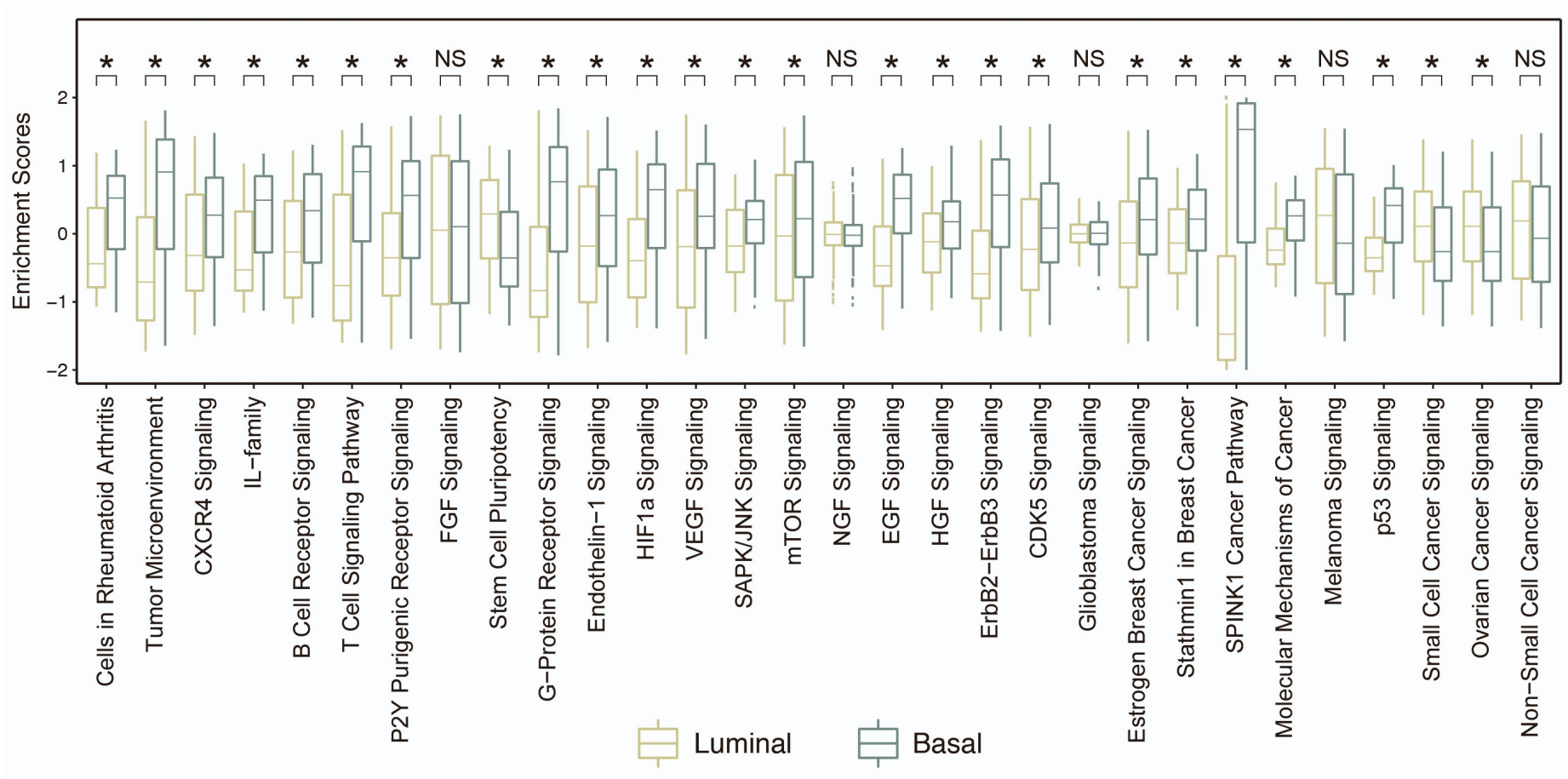

Figure S22. The box plot analysis of the enrichment scores of the regulons controlling immunity, inflammation, signal transduction/differentiation, and oncogenesis in molecular subtypes in the TCGA cohort, related to Figure 8. Asterisks indicate statistically significant difference (p value <0.05) based on Wilcoxon rank-sum test; NS, not significant difference (p value≥0.05).

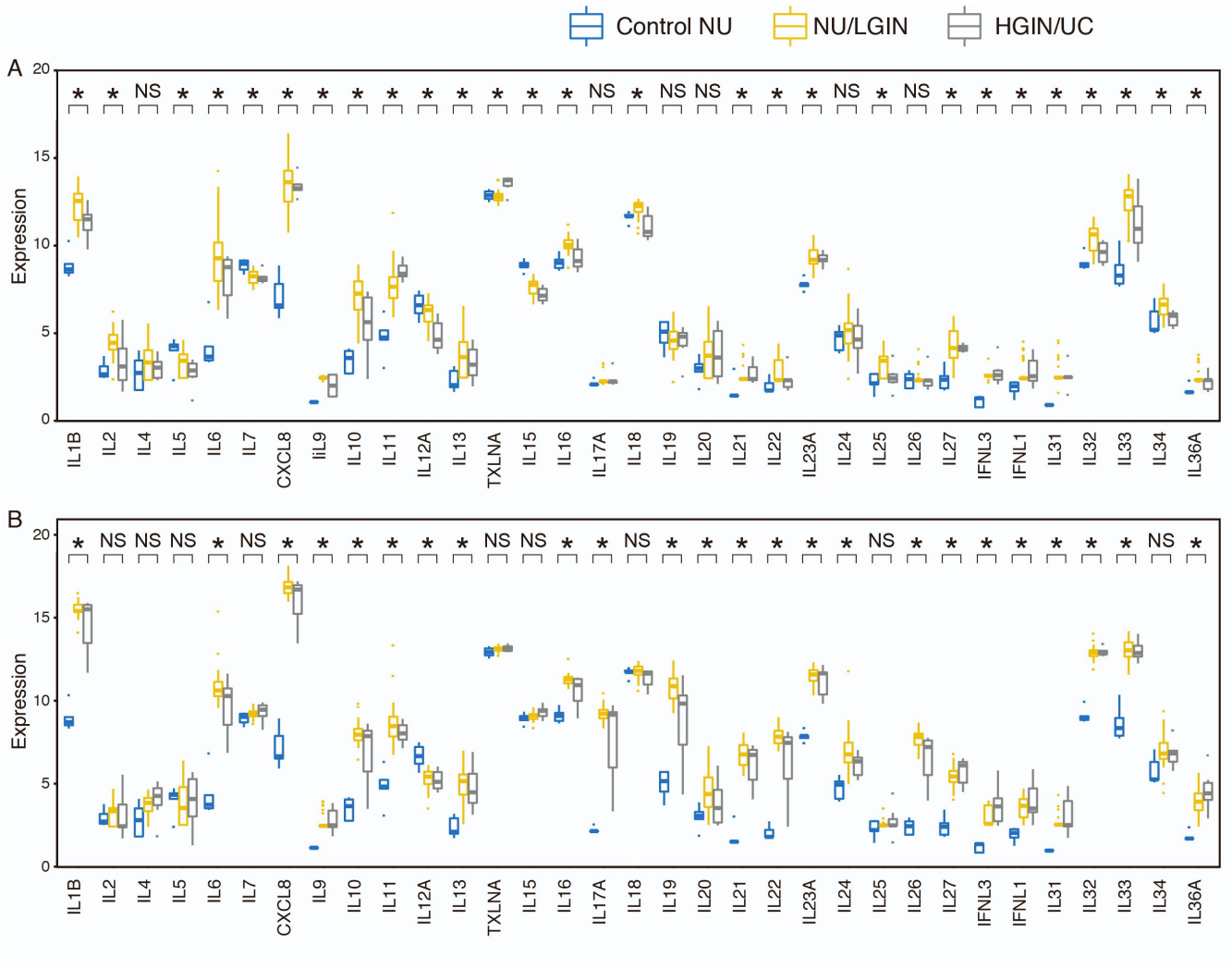

Figure S23. The box plot analysis of the expression levels of interleukins in the two groups of mucosal samples of NU/LGIN and HGIN/UC compared to control NU, related to Figure 8. (A) Expression levels of interleukins in a luminal map. **(B)** Expression levels of interleukins in a basal map. Asterisks indicate statistically significant difference (p value <0.05) based on ANOVA F-test; NS, not significant difference (p value ≥0.05).

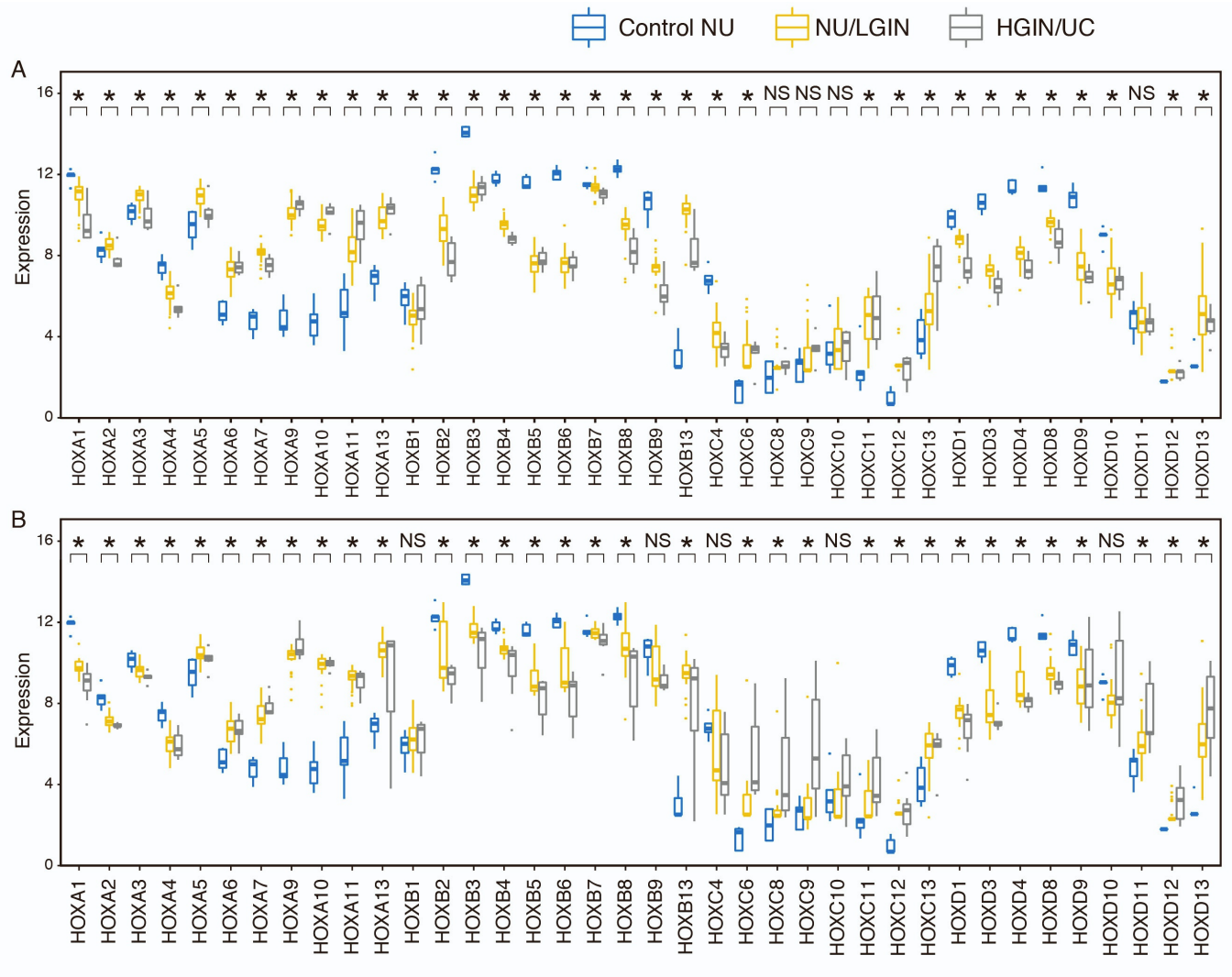

Figure S24. The box plot analysis of the expression levels of the HOX genes in the two groups of mucosal samples of NU/LGIN and HGIN/UC compared to control NU, related to Figure 8. (A) Expression levels of the HOX genes in a luminal map. **(B)** Expression levels of the HOX genes in a basal map. Asterisks indicate statistically significant difference (p value <0.05) based on ANOVA F-test; NS, not significant difference (p value ≥0.05).

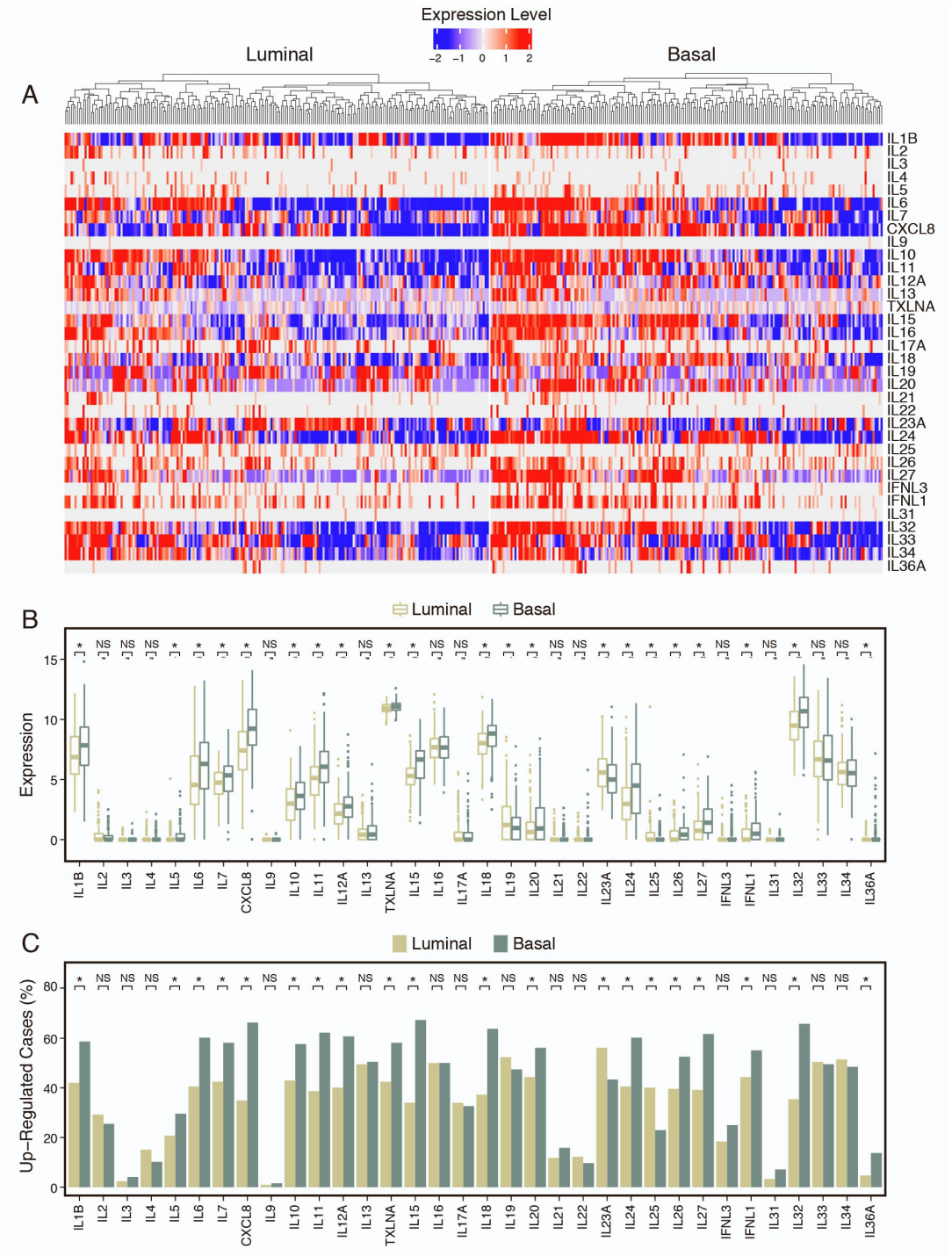

Figure S25. Expression patterns for all interleukins validated in the TCGA cohort, related to Figure 8. (A) Expression pattern of the interleukins in the luminal and basal bladder cancers. **(B)** The box plot analysis of interleukins expression levels in the luminal and basal bladder cancers. **(C)** The proportion of luminal and basal bladder cancer cases with upregulated interleukins. Asterisks indicate statistically significant difference (p value<0.05) based on Wilcoxon rank-sum test **(B)** and chi-squared test **(C)**; NS, not significant difference (p value ≥0.05).

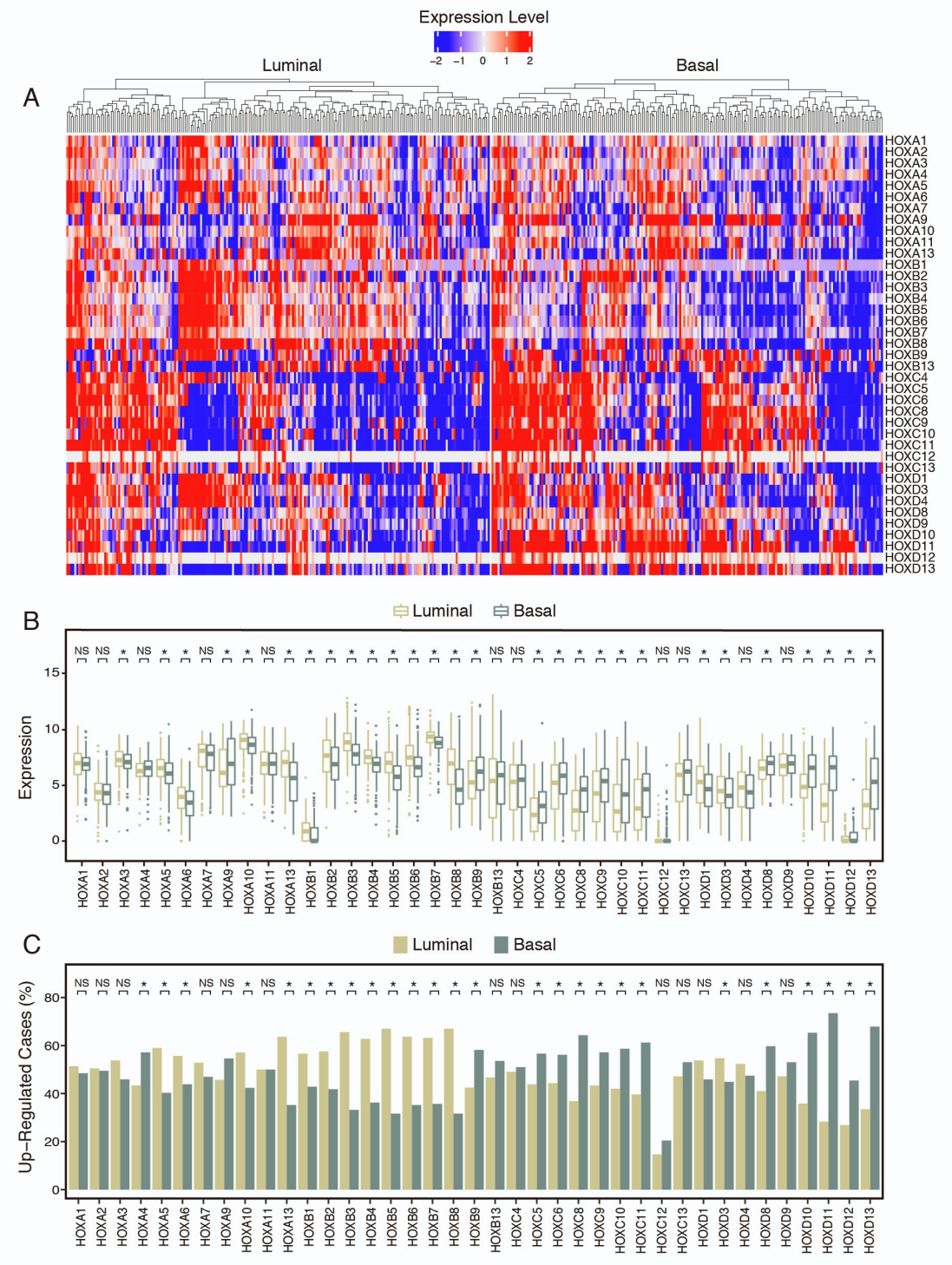

Figure S26. Expression patterns for all HOX genes validated in the TCGA cohort, related to Figure 8. (A) Expression pattern of the HOX genes in the luminal and basal bladder cancers. **(B)** The box plot analysis of the HOX genes expression levels in the luminal and basal bladder cancers. **(C)** The proportion of luminal and basal bladder cancer cases with the upregulated HOX genes. Asterisks indicate statistically significant difference (p value <0.05) based on Wilcoxon rank-sum test **(B)** and chi-squared test **(C)**; NS, not significant difference (p value ≥0.05).

Table S1.Summary of clinical and pathological characterization of cystectomy specimens, related to Figure 1

	Map #	Age	Origin	Gender	Occupation	Smoking Status	Alcohol and Drugs	Other Diseases	Family History	Histologic al Type of BC	Stage	Grade	Molecular Type of BC	Growth	Number of samples collected								
															NU/LGIN			NU/LGIN	HGIN		HGIN	UC	All samples
															NU	MD	MdD		SD	CIS			
1	16	71	Caucasian	M	Retired military	Never smoker	Occasional alcohol	Arthritis	Brother with pancreatic cancer	UC	T4	High	B	Non-papillary	21	18	5	44	13	7	20	14	78
2	17	80	Caucasian	M	Educational consultant	Former smoker	1-2 glasses of wine per day	Coronary artery disease, lip cancer, Parkinson disease	Brother with kidney cancer	UC	T2	High	B	Non-papillary	16	5	0	21	0	18	18	1	40
3	18	81	Caucasian	M	Retired military	Former smoker	None	Pneumonia, stroke, dementia	Father with skin cancer	UC	T3	High	L	Papillary	0	1	4	5	2	18	20	30	55
4	19	86	Caucasian	M	Retiree	Former smoker	None	Prostate cancer, aortic aneurysm, pulmonary embolus	None	UC	T3	High	B	Non-papillary	13	9	9	31	4	0	4	9	44
5	20	55	Caucasian	M	Lumber company worker	Former smoker	Occasional alcohol	None	None	UC	T2	High	L	Papillary	14	13	11	38	2	0	2	2	42
6	21	69	Caucasian	M	Reiterd computer analist	Never smoker	None	Hypertension	Mother with liver cancer	UC	T3	High	L	Non-papillary	7	9	13	29	1	0	1	15	45
7	22	73	Caucasian	M	Retired teacher	Current smoker	None	Coronary artery disease	None	UC	T3	High	L	Non-papillary	0	3	6	9	5	13	18	7	34
8	23	79	Caucasian	M	Retired mill worker	Former smoker	None	Diabetes, hypertension	Son with rectal cancer	UC	T2	High	L	Papillary	8	7	7	22	1	0	1	18	41
9	24	68	Caucasian	M	Home builder	Former smoker	2 glasses of wine per day	Hypertension, glaucoma	Mother with breast cancer	UC	T3	High	L	Non-papillary	32	4	8	44	3	3	6	4	54
Total															111	69	63	243	31	59	90	100	433

BC, bladder cancer; M, male; UC, urothelial carcinoma; B, basal; L, luminal; NU, normal urothelium; MD, mild dysplesia; MdD, moderate dysplasia; CIS, carcinoma *in situ*; LGIN, low grade intraurothelial neoplasia; HGIN, high grade intraurothelial neoplasia

Table S2. Number of Dysregulated Genes (RNASeq and Methylation) in Luminal (Map 24) and Basal (Map 19) Maps, related to Figure 2

	MAP 24 (Luminal)			MAP 19 (Basal)		
	Number of Altered Genes			**Number of Altered Genes**		
	NU/LGIN	HGIN,UC		NU/LGIN	HGIN, UC	
RNAseq			**Total**			**Total**
Upregulated	1245	1067		2017	859	
Downregulated	163	864		362	327	
Subtotal	1408	1931	[3339]	2379	1186	[3565]
Methylation			**Total**			**Total**
Hypermethylated	56	340		254	995	
Hypomethylated	69	915		173	236	
Total	125	1255	[1380]	427	1231	[1658]

Table S3. Summary of Mutations Identified in Luminal and Basal Cystectomy Specimens, related to Figure 6

	Luminal (MAP24)	Basal (MAP19)
Cluster A		
Non-silent mutations	1303	2176
SNV	1250	1924
Insertions	10	29
Deletions	43	223
Cluster B		
Non-silent mutations	76	511
SNV	74	475
Insertions	1	6
Deletions	1	30
Cluster α		
Non-silent mutations	80	43
SNV	77	41
Insertions	1	0
Deletions	2	2
Cluster β		
Non-silent mutations	77	155
SNV	75	147
Insertions	1	1
Deletions	1	7

Table S4. List of Mutations in Cluster Alpha in the Luminal Map (Map 24), related to Figure 6

	Mutation	Chr	Start	End	Ref	Alt	Protein_Change	Variant_Classification	Effect	Mut_Type	Mut_ID
1	TMEM163:chr2:134718832	chr2	134718832	134718832	G	A	p.P35L	Missense_Mutation	nonsilent	SNV	TMEM163:chr2:134718832
2	PACS1:chr11:66070590	chr11	66070590	66070590	A	C	p.Q35P	Missense_Mutation	nonsilent	SNV	PACS1:chr11:66070590
3	ASB15:chr7:123617707	chr7	123617707	123617707	A	C	p.N141H	Missense_Mutation	nonsilent	SNV	ASB15:chr7:123617707
4	ASB15:chr7:123617682	chr7	123617682	123617682	A	C	p.E132D	Missense_Mutation	nonsilent	SNV	ASB15:chr7:123617682
5	PCDH10:chr4:133152499	chr4	133152499	133152499	A	C	p.I787L	Missense_Mutation	nonsilent	SNV	PCDH10:chr4:133152499
6	WDR33:chr2:127726703	chr2	127726703	127726703	G	A	p.Q267*	Nonsense_Mutation	null	SNV	WDR33:chr2:127726703
7	MBTPS1:chr16:84091800	chr16	84091800	84091800	T	G	p.K299Q	Missense_Mutation	nonsilent	SNV	MBTPS1:chr16:84091800
8	UGT1A4:chr2:233718899	chr2	233718899	233718899	G	T	p.E27*	Nonsense_Mutation	null	SNV	UGT1A4:chr2:233718899
9	UGT1A4:chr2:233719010	chr2	233719010	233719010	G	A	p.E64K	Missense_Mutation	nonsilent	SNV	UGT1A4:chr2:233719010
10	RECQL:chr12:21470988	chr12	21470988	21470988	G	A	p.S593F	Missense_Mutation	nonsilent	SNV	RECQL:chr12:21470988
11	OTOP1:chr4:4197744	chr4	4197744	4197744	C	T	p.A364T	Missense_Mutation	nonsilent	SNV	OTOP1:chr4:4197744
12	VSIG2:chr11:124750891	chr11	124750891	124750891	G	A	p.P84S	Missense_Mutation	nonsilent	SNV	VSIG2:chr11:124750891
13	SEPT14:chr7:55842957	chr7	55842957	55842957	C	A	p.K181N	Missense_Mutation	nonsilent	SNV	SEPT14:chr7:55842957
14	MARVELD3:chr16:71626363	chr16	71626363	71626363	G	A	p.R45Q	Missense_Mutation	nonsilent	SNV	MARVELD3:chr16:71626363
15	RB1:chr13:48465295	chr13	48465295	48465296	-	T	p.S807fs	Frame_Shift_Ins	null	Insertion	RB1:chr13:48465295
16	PKDREJ:chr22:46262713	chr22	46262713	46262713	C	T	p.V204I	Missense_Mutation	nonsilent	SNV	PKDREJ:chr22:46262713
17	CSDE1:chr1:114733742	chr1	114733742	114733742	C	T	p.S146N	Missense_Mutation	nonsilent	SNV	CSDE1:chr1:114733742
18	PLCB3:chr11:64267452	chr11	64267452	64267452	G	A	p.D1201N	Missense_Mutation	nonsilent	SNV	PLCB3:chr11:64267452
19	KITLG:chr12:88518810	chr12	88518810	88518810	G	A	p.L84F	Missense_Mutation	nonsilent	SNV	KITLG:chr12:88518810
20	CNBD1:chr8:87353727	chr8	87353727	87353727	G	A	p.C415Y	Missense_Mutation	nonsilent	SNV	CNBD1:chr8:87353727
21	IRS2:chr13:109785170	chr13	109785170	109785170	T	A	p.K295M	Missense_Mutation	nonsilent	SNV	IRS2:chr13:109785170
22	MMP1:chr11:102795539	chr11	102795539	102795539	T	C	p.I232V	Missense_Mutation	nonsilent	SNV	MMP1:chr11:102795539
23	TPTE:chr21:10596087	chr21	10596087	10596087	C	T	p.R426C	Splice_Site	null	SNV	TPTE:chr21:10596087
24	SNAPC4:chr9:136381953	chr9	136381953	136381953	G	A	p.R730C	Missense_Mutation	nonsilent	SNV	SNAPC4:chr9:136381953
25	PCDHB16:chr5:141184457	chr5	141184457	141184457	G	T	p.R633L	Missense_Mutation	nonsilent	SNV	PCDHB16:chr5:141184457
26	TRAK2:chr2:201386338	chr2	201386338	201386338	C	T	p.E615K	Missense_Mutation	nonsilent	SNV	TRAK2:chr2:201386338
27	OR1E1:chr17:3397615	chr17	3397615	3397615	T	C	p.S266G	Missense_Mutation	nonsilent	SNV	OR1E1:chr17:3397615
28	IMPG1:chr6:75931152	chr6	75931152	75931152	C	A	NA	Splice_Site	null	SNV	IMPG1:chr6:75931152
29	VSIG1:chrX:108067099	chrX	108067099	108067099	G	A	p.G126D	Missense_Mutation	nonsilent	SNV	VSIG1:chrX:108067099
30	SAMSN1:chr21:14498592	chr21	14498592	14498592	C	A	p.E257*	Splice_Site	null	SNV	SAMSN1:chr21:14498592
31	GPR142:chr17:74372090	chr17	74372090	74372090	C	G	p.F293L	Missense_Mutation	nonsilent	SNV	GPR142:chr17:74372090
32	SIX4:chr14:60720380	chr14	60720380	60720380	T	C	p.H310R	Missense_Mutation	nonsilent	SNV	SIX4:chr14:60720380
33	MYH4:chr17:10457566	chr17	10457566	10457566	T	C	p.H584R	Missense_Mutation	nonsilent	SNV	MYH4:chr17:10457566
34	KRTAP5-7:chr11:71527659	chr11	71527659	71527659	G	A	p.C120Y	Missense_Mutation	nonsilent	SNV	KRTAP5-7:chr11:71527659
35	INHBB:chr2:120349204	chr2	120349204	120349204	T	A	p.L185Q	Missense_Mutation	nonsilent	SNV	INHBB:chr2:120349204
36	MUC16:chr19:8885277	chr19	8885277	8885277	C	G	NA	Splice_Site	null	SNV	MUC16:chr19:8885277
37	ITGA7:chr12:55694808	chr12	55694808	55694808	G	T	p.H722Q	Missense_Mutation	nonsilent	SNV	ITGA7:chr12:55694808
38	ZNF574:chr19:42080798	chr19	42080798	42080798	C	G	p.A731G	Missense_Mutation	nonsilent	SNV	ZNF574:chr19:42080798
39	C12orf66:chr12:64194197	chr12	64194197	64194197	T	A	p.H328L	Missense_Mutation	nonsilent	SNV	C12orf66:chr12:64194197
40	COPS5:chr8:67059360	chr8	67059360	67059360	C	T	p.V13M	Missense_Mutation	nonsilent	SNV	COPS5:chr8:67059360
41	POU2AF1:chr11:111357545	chr11	111357545	111357545	G	A	p.S119L	Missense_Mutation	nonsilent	SNV	POU2AF1:chr11:111357545
42	OPRD1:chr1:28862856	chr1	28862856	28862856	T	A	p.V231E	Missense_Mutation	nonsilent	SNV	OPRD1:chr1:28862856
43	RPGRIP1L:chr16:53637725	chr16	53637725	53637725	T	C	p.T1030A	Missense_Mutation	nonsilent	SNV	RPGRIP1L:chr16:53637725
44	SASH1:chr6:148544104	chr6	148544104	148544104	G	C	p.K878N	Missense_Mutation	nonsilent	SNV	SASH1:chr6:148544104
45	IGFN1:chr1:201206758	chr1	201206758	201206758	C	T	p.P622L	Missense_Mutation	nonsilent	SNV	IGFN1:chr1:201206758
46	ATG4C:chr1:62834116	chr1	62834116	62834116	G	C	p.D338H	Splice_Site	null	SNV	ATG4C:chr1:62834116
47	C11orf80:chr11:66756380	chr11	66756380	66756380	C	T	p.P66L	Missense_Mutation	nonsilent	SNV	C11orf80:chr11:66756380
48	MYO18B:chr22:25823622	chr22	25823622	25823622	A	T	p.Q880L	Missense_Mutation	nonsilent	SNV	MYO18B:chr22:25823622
49	CEACAM7:chr19:41677414	chr19	41677414	41677414	A	G	p.*266Q	Nonstop_Mutation	null	SNV	CEACAM7:chr19:41677414
50	ZAP70:chr2:97732905	chr2	97732905	97732918	GGCACATACGCCT	-	p.G196fs	Frame_Shift_Del	null	Deletion	ZAP70:chr2:97732905
51	SH3RF2:chr5:146013951	chr5	146013951	146013951	G	A	p.G317R	Missense_Mutation	nonsilent	SNV	SH3RF2:chr5:146013951
52	DPYD:chr1:97549639	chr1	97549639	97549639	A	G	p.V482A	Missense_Mutation	nonsilent	SNV	DPYD:chr1:97549639
53	NCAPG2:chr7:158652293	chr7	158652293	158652293	C	A	p.R978R	Splice_Site	null	SNV	NCAPG2:chr7:158652293
54	FGF10:chr5:44388576	chr5	44388576	44388576	G	A	p.T36I	Missense_Mutation	nonsilent	SNV	FGF10:chr5:44388576
55	FAT3:chr11:92840649	chr11	92840649	92840649	A	G	p.I3336V	Missense_Mutation	nonsilent	SNV	FAT3:chr11:92840649
56	TNN:chr1:175077743	chr1	175077743	175077743	C	A	p.L109M	Missense_Mutation	nonsilent	SNV	TNN:chr1:175077743
57	GNAS:chr20:58854895	chr20	58854895	58854895	C	T	p.R544W	Missense_Mutation	nonsilent	SNV	GNAS:chr20:58854895
58	USP8:chr15:50495917	chr15	50495917	50495917	G	A	p.A804T	Missense_Mutation	nonsilent	SNV	USP8:chr15:50495917
59	GRXCR2:chr5:145866507	chr5	145866507	145866507	A	C	p.Y186*	Nonsense_Mutation	null	SNV	GRXCR2:chr5:145866507
60	TBL1Y:chrY:7063918	chrY	7063918	7063918	C	T	p.R76C	Missense_Mutation	nonsilent	SNV	TBL1Y:chrY:7063918
61	PIGB:chr15:55350844	chr15	55350844	55350844	C	A	p.Y423*	Nonsense_Mutation	null	SNV	PIGB:chr15:55350844
62	RNF32:chr7:156675744	chr7	156675744	156675744	G	T	p.E245*	Nonsense_Mutation	null	SNV	RNF32:chr7:156675744
63	OR5M10:chr11:56577516	chr11	56577516	56577516	A	G	p.V69A	Missense_Mutation	nonsilent	SNV	OR5M10:chr11:56577516
64	ADGB:chr6:146764102	chr6	146764102	146764102	T	C	NA	Splice_Site	null	SNV	ADGB:chr6:146764102
65	ZNF645:chrX:22274249	chrX	22274249	22274249	A	G	p.R420G	Missense_Mutation	nonsilent	SNV	ZNF645:chrX:22274249
66	ABCC9:chr12:21817195	chr12	21817195	21817195	C	T	p.G1295D	Missense_Mutation	nonsilent	SNV	ABCC9:chr12:21817195
67	DSG4:chr18:31411348	chr18	31411348	31411348	C	G	p.A752G	Missense_Mutation	nonsilent	SNV	DSG4:chr18:31411348
68	SLC27A6:chr5:129016036	chr5	129016036	129016036	C	T	p.T374I	Missense_Mutation	nonsilent	SNV	SLC27A6:chr5:129016036
69	FAM199X:chrX:104188281	chrX	104188281	104188281	C	A	p.A324E	Missense_Mutation	nonsilent	SNV	FAM199X:chrX:104188281
70	ASXL3:chr18:33740213	chr18	33740213	33740213	T	A	p.S937T	Missense_Mutation	nonsilent	SNV	ASXL3:chr18:33740213
71	KRT71:chr12:52548701	chr12	52548701	52548701	G	A	p.A271A	Splice_Site	null	SNV	KRT71:chr12:52548701
72	DOCK7:chr1:62578916	chr1	62578916	62578916	G	T	p.T641N	Missense_Mutation	nonsilent	SNV	DOCK7:chr1:62578916
73	CACNA1A:chr19:13208878	chr19	13208878	13208880	GAT	-	p.H2219del	In_Frame_Del	null	Deletion	CACNA1A:chr19:13208878
74	MUC6:chr11:1016770	chr11	1016770	1016770	G	A	p.P2011S	Missense_Mutation	nonsilent	SNV	MUC6:chr11:1016770
75	KIF18A:chr11:28088712	chr11	28088712	28088712	G	A	p.R237*	Nonsense_Mutation	null	SNV	KIF18A:chr11:28088712
76	NRXN1:chr2:50053527	chr2	50053527	50053527	T	G	p.Q1331P	Missense_Mutation	nonsilent	SNV	NRXN1:chr2:50053527
77	FAM47A:chrX:34130558	chrX	34130558	34130558	T	A	p.K574M	Missense_Mutation	nonsilent	SNV	FAM47A:chrX:34130558
78	FAXC:chr6:99323536	chr6	99323536	99323536	C	T	p.R244H	Missense_Mutation	nonsilent	SNV	FAXC:chr6:99323536
79	DNAH9:chr17:11854013	chr17	11854013	11854013	C	A	p.T3173K	Missense_Mutation	nonsilent	SNV	DNAH9:chr17:11854013
80	RASGRF1:chr15:79058468	chr15	79058468	79058468	C	T	p.A133T	Missense_Mutation	nonsilent	SNV	RASGRF1:chr15:79058468

Table S5. List of Mutations in Cluster Alpha in the Basal Map (Map 19), related to Figure 6

	Mutation	Chr	Start	End	Ref	Alt	Protein_Change	Variant_Classification	Effect	Mut_Type	Mut_ID
1	FLNC:chr7:128842686	chr7	128842686	128842686	G	T	p.E793*	Nonsense_Mutation	null	SNV	FLNC:chr7:128842686
2	ERCC2:chr19:45364429	chr19	45364429	45364429	T	C	p.N238S	Missense_Mutation	nonsilent	SNV	ERCC2:chr19:45364429
3	TIMMDC1:chr3:119498789	chr3	119498789	119498789	T	G	p.F19C	Missense_Mutation	nonsilent	SNV	TIMMDC1:chr3:119498789
4	VCX3B:chrX:8466330	chrX	8466330	8466330	A	G	p.M230V	Missense_Mutation	nonsilent	SNV	VCX3B:chrX:8466330
5	ZMIZ1:chr10:79292307	chr10	79292307	79292307	T	A	p.V303E	Missense_Mutation	nonsilent	SNV	ZMIZ1:chr10:79292307
6	CACNB2:chr10:18538203	chr10	18538203	18538203	T	G	p.D414E	Missense_Mutation	nonsilent	SNV	CACNB2:chr10:18538203
7	SPAG1:chr8:100220398	chr8	100220398	100220398	G	A	p.C552Y	Missense_Mutation	nonsilent	SNV	SPAG1:chr8:100220398
8	PRR22:chr19:5783829	chr19	5783829	5783829	G	C	p.P140A	Missense_Mutation	nonsilent	SNV	PRR22:chr19:5783829
9	LRRK2:chr12:40259572	chr12	40259572	40259572	C	T	p.A504V	Missense_Mutation	nonsilent	SNV	LRRK2:chr12:40259572
10	IWS1:chr2:127505742	chr2	127505742	127505742	C	A	p.S54I	Missense_Mutation	nonsilent	SNV	IWS1:chr2:127505742
11	ACIN1:chr14:23080168	chr14	23080168	23080169	-	G	p.V448fs	Frame_Shift_Ins	null	Insertion	ACIN1:chr14:23080168
12	XKR6:chr8:11200724	chr8	11200724	11200725	-	G	p.M206fs	Frame_Shift_Ins	null	Insertion	XKR6:chr8:11200724
13	WDHD1:chr14:54944459	chr14	54944459	54944459	C	T	p.G1021E	Missense_Mutation	nonsilent	SNV	WDHD1:chr14:54944459
14	CLMN:chr14:95203283	chr14	95203283	95203283	C	T	p.S689N	Missense_Mutation	nonsilent	SNV	CLMN:chr14:95203283
15	SERPINA3:chr14:94619419	chr14	94619419	94619420	AT	CA	p.M290Q	Missense_Mutation	nonsilent	SNV	SERPINA3:chr14:94619419
16	RP11-51L5.4:chr17:62260772	chr17	62260772	62260772	A	G	NA	Splice_Site	null	SNV	RP11-51L5.4:chr17:62260772
17	RP11-402P6.15:chrX:71670304	chrX	71670304	71670305	GC	AT	p.Q481*	Nonsense_Mutation	null	SNV	RP11-402P6.15:chrX:71670304
18	RP11-402P6.15:chrX:71668128	chrX	71668128	71668128	C	A	p.P109T	Missense_Mutation	nonsilent	SNV	RP11-402P6.15:chrX:71668128
19	RP11-402P6.15:chrX:71668120	chrX	71668120	71668120	C	T	p.A106V	Missense_Mutation	nonsilent	SNV	RP11-402P6.15:chrX:71668120
20	PPIP5K1:chr15:43536239	chr15	43536239	43536240	CA	TG	p.C1105H	Missense_Mutation	nonsilent	SNV	PPIP5K1:chr15:43536239
21	OR1S1:chr11:58215638	chr11	58215638	58215638	A	G	p.I285M	Missense_Mutation	nonsilent	SNV	OR1S1:chr11:58215638
22	OR7E36P:chr13:41431248	chr13	41431248	41431249	-	AAG	NA	Splice_Site	null	Insertion	OR7E36P:chr13:41431248
23	OR1S1:chr11:58215047	chr11	58215047	58215047	G	C	p.K88N	Missense_Mutation	nonsilent	SNV	OR1S1:chr11:58215047
24	OTOG:chr11:17593745	chr11	17593745	17593745	C	T	p.P1093S	Missense_Mutation	nonsilent	SNV	OTOG:chr11:17593745
25	TNFRSF14:chr1:2561679	chr1	2561679	2561679	C	G	p.S186R	Missense_Mutation	nonsilent	SNV	TNFRSF14:chr1:2561679
26	KIAA1671:chr22:25177409	chr22	25177409	25177409	G	A	p.R1654H	Missense_Mutation	nonsilent	SNV	KIAA1671:chr22:25177409
27	GRIP2:chr3:14540271	chr3	14540271	14540271	G	A	p.A13V	Missense_Mutation	nonsilent	SNV	GRIP2:chr3:14540271
28	DIP2C:chr10:399191	chr10	399191	399191	G	A	p.P393L	Missense_Mutation	nonsilent	SNV	DIP2C:chr10:399191
29	RNF34:chr12:121416160	chr12	121416160	121416160	C	T	p.A3V	Splice_Site	null	SNV	RNF34:chr12:121416160
30	SF3B1:chr2:197400743	chr2	197400743	197400743	A	C	p.L897R	Missense_Mutation	nonsilent	SNV	SF3B1:chr2:197400743
31	STKLD1:chr9:133403800	chr9	133403800	133403800	C	A	p.C525*	Nonsense_Mutation	null	SNV	STKLD1:chr9:133403800
32	ZNF318:chr6:43368972	chr6	43368972	43368979	TGCCGCTG	-	p.D129fs	Frame_Shift_Del	null	Deletion	ZNF318:chr6:43368972
33	ARSE:chrX:2949610	chrX	2949610	2949610	C	T	p.R183H	Missense_Mutation	nonsilent	SNV	ARSE:chrX:2949610
34	RP11-683L23.1:chr18:48009	chr18	48009	48009	C	T	p.C239Y	Missense_Mutation	nonsilent	SNV	RP11-683L23.1:chr18:48009
35	CLDN9:chr16:3013447	chr16	3013447	3013447	C	A	p.L29M	Missense_Mutation	nonsilent	SNV	CLDN9:chr16:3013447
36	ZC3H7B:chr22:41320707	chr22	41320707	41320707	T	A	p.F16Y	Missense_Mutation	nonsilent	SNV	ZC3H7B:chr22:41320707
37	ARAP2:chr4:36148419	chr4	36148419	36148419	C	A	p.E996*	Nonsense_Mutation	null	SNV	ARAP2:chr4:36148419
38	RBMXL3:chrX:115191182	chrX	115191182	115191183	CA	TG	p.Q581W	Missense_Mutation	nonsilent	SNV	RBMXL3:chrX:115191182
39	RBMXL3:chrX:115191188	chrX	115191188	115191188	A	C	p.N583H	Missense_Mutation	nonsilent	SNV	RBMXL3:chrX:115191188
40	TMED7:chr5:115625789	chr5	115625789	115625789	G	A	p.P2S	Missense_Mutation	nonsilent	SNV	TMED7:chr5:115625789
41	SLC27A6:chr5:129029625	chr5	129029625	129029625	C	A	p.T534K	Missense_Mutation	nonsilent	SNV	SLC27A6:chr5:129029625
42	LGSN:chr6:63280565	chr6	63280565	63280565	C	A	p.C329F	Missense_Mutation	nonsilent	SNV	LGSN:chr6:63280565
43	EIF3D:chr22:36519493	chr22	36519493	36519493	C	T	p.R208H	Missense_Mutation	nonsilent	SNV	EIF3D:chr22:36519493

Table S6. List of Mutations in Cluster Beta in the Luminal Map (Map 24), related to Figure 6

	Mutation	Chr	Start	End	Ref	Alt	Protein_Change	Variant_Classification	Effect	Mut_Type	Mut_ID
1	MAGEA4:chrX:151924617	chrX	1.52E+08	1.52E+08	G	C	p.*318S	Nonstop_Mutation	null	SNV	MAGEA4:chrX:151924617
2	EMC9:chr14:24139634	chr14	24139634	24139634	G	C	p.L12V	Missense_Mutation	nonsilent	SNV	EMC9:chr14:24139634
3	SCUBE2:chr11:9047414	chr11	9047414	9047415	TG	-	p.T648fs	Frame_Shift_Del	null	Deletion	SCUBE2:chr11:9047414
4	BAP1:chr3:52403766	chr3	52403766	52403766	G	C	p.S460*	Nonsense_Mutation	null	SNV	BAP1:chr3:52403766
5	NEUROD1:chr2:181678217	chr2	1.82E+08	1.82E+08	G	C	p.P215R	Missense_Mutation	nonsilent	SNV	NEUROD1:chr2:181678217
6	NCAM1:chr11:113255947	chr11	1.13E+08	1.13E+08	C	G	p.I623M	Missense_Mutation	nonsilent	SNV	NCAM1:chr11:113255947
7	C5orf42:chr5:37226683	chr5	37226683	37226683	G	T	p.Q638K	Missense_Mutation	nonsilent	SNV	C5orf42:chr5:37226683
8	TMEFF1:chr9:100572613	chr9	1.01E+08	1.01E+08	T	C	p.I332T	Missense_Mutation	nonsilent	SNV	TMEFF1:chr9:100572613
9	ADAMTSL1:chr9:18622334	chr9	18622334	18622334	G	A	p.R189Q	Missense_Mutation	nonsilent	SNV	ADAMTSL1:chr9:18622334
10	GLRA1:chr5:151851604	chr5	1.52E+08	1.52E+08	C	G	p.G233A	Splice_Site	null	SNV	GLRA1:chr5:151851604
11	ABCC8:chr11:17413399	chr11	17413399	17413399	C	T	p.E824K	Missense_Mutation	nonsilent	SNV	ABCC8:chr11:17413399
12	APC:chr5:112839465	chr5	1.13E+08	1.13E+08	C	T	p.Q1291*	Nonsense_Mutation	null	SNV	APC:chr5:112839465
13	IRAK1:chrX:154019788	chrX	1.54E+08	1.54E+08	C	T	p.E9K	Missense_Mutation	nonsilent	SNV	IRAK1:chrX:154019788
14	BSN:chr3:49651075	chr3	49651075	49651075	C	A	p.A661E	Missense_Mutation	nonsilent	SNV	BSN:chr3:49651075
15	DGAT2:chr11:75798366	chr11	75798366	75798366	C	T	p.R317*	Nonsense_Mutation	null	SNV	DGAT2:chr11:75798366
16	ALOX5:chr10:45443465	chr10	45443465	45443465	G	C	p.E501Q	Missense_Mutation	nonsilent	SNV	ALOX5:chr10:45443465
17	PCDH9:chr13:66304893	chr13	66304893	66304893	G	A	p.S1159L	Missense_Mutation	nonsilent	SNV	PCDH9:chr13:66304893
18	FPR1:chr19:51746492	chr19	51746492	51746492	G	A	p.P168L	Missense_Mutation	nonsilent	SNV	FPR1:chr19:51746492
19	C10orf71:chr10:49324658	chr10	49324658	49324658	G	A	p.E705K	Missense_Mutation	nonsilent	SNV	C10orf71:chr10:49324658
20	CDKN1A:chr6:36684429	chr6	36684429	36684430	-	A	p.H110fs	Frame_Shift_Ins	null	Insertion	CDKN1A:chr6:36684429
21	ADAMTS17:chr15:99997486	chr15	99997486	99997486	C	T	p.A899T	Missense_Mutation	nonsilent	SNV	ADAMTS17:chr15:99997486
22	USP28:chr11:113823688	chr11	1.14E+08	1.14E+08	C	G	p.R400S	Missense_Mutation	nonsilent	SNV	USP28:chr11:113823688
23	MUC5B:chr11:1248411	chr11	1248411	1248411	C	A	p.T3844N	Missense_Mutation	nonsilent	SNV	MUC5B:chr11:1248411
24	PRRC2A:chr6:31632385	chr6	31632385	31632385	G	C	p.E1238Q	Missense_Mutation	nonsilent	SNV	PRRC2A:chr6:31632385
25	C5orf42:chr5:37226785	chr5	37226785	37226785	G	A	p.H604Y	Missense_Mutation	nonsilent	SNV	C5orf42:chr5:37226785
26	FIGN:chr2:163610118	chr2	1.64E+08	1.64E+08	G	T	p.L572I	Missense_Mutation	nonsilent	SNV	FIGN:chr2:163610118
27	UGGT1:chr2:128113209	chr2	1.28E+08	1.28E+08	C	G	p.S216*	Nonsense_Mutation	null	SNV	UGGT1:chr2:128113209
28	ITGAV:chr2:186625495	chr2	1.87E+08	1.87E+08	G	A	p.W144*	Nonsense_Mutation	null	SNV	ITGAV:chr2:186625495
29	CROCC:chr1:16966080	chr1	16966080	16966080	G	A	p.A1553T	Missense_Mutation	nonsilent	SNV	CROCC:chr1:16966080
30	XPO7:chr8:22003299	chr8	22003299	22003299	G	C	p.L1008F	Missense_Mutation	nonsilent	SNV	XPO7:chr8:22003299
31	ZCCHC11:chr1:52481843	chr1	52481843	52481843	C	G	p.Q532H	Missense_Mutation	nonsilent	SNV	ZCCHC11:chr1:52481843
32	PLA2G4D:chr15:42070059	chr15	42070059	42070059	C	T	p.G694R	Missense_Mutation	nonsilent	SNV	PLA2G4D:chr15:42070059
33	SCAPER:chr15:76348651	chr15	76348651	76348651	C	G	p.L1395F	Missense_Mutation	nonsilent	SNV	SCAPER:chr15:76348651
34	HERC1:chr15:63666389	chr15	63666389	63666389	G	C	p.L2764V	Missense_Mutation	nonsilent	SNV	HERC1:chr15:63666389
35	ADAM12:chr10:126049362	chr10	1.26E+08	1.26E+08	G	A	p.P606L	Missense_Mutation	nonsilent	SNV	ADAM12:chr10:126049362
36	MAS1:chr6:159907088	chr6	1.6E+08	1.6E+08	G	A	p.V45M	Missense_Mutation	nonsilent	SNV	MAS1:chr6:159907088
37	GPR63:chr6:96798634	chr6	96798634	96798634	C	G	p.L366F	Missense_Mutation	nonsilent	SNV	GPR63:chr6:96798634
38	ENPEP:chr4:110476761	chr4	1.1E+08	1.1E+08	C	T	p.T116M	Missense_Mutation	nonsilent	SNV	ENPEP:chr4:110476761
39	FBXW7:chr4:152337818	chr4	1.52E+08	1.52E+08	G	C	p.S202*	Nonsense_Mutation	null	SNV	FBXW7:chr4:152337818
40	PPP1R12A:chr12:79795669	chr12	79795669	79795669	C	T	p.R851K	Missense_Mutation	nonsilent	SNV	PPP1R12A:chr12:79795669
41	GLTSCR2:chr19:47755416	chr19	47755416	47755416	C	G	p.I374M	Missense_Mutation	nonsilent	SNV	GLTSCR2:chr19:47755416
42	SCARF1:chr17:1643670	chr17	1643670	1643670	C	T	p.R188H	Missense_Mutation	nonsilent	SNV	SCARF1:chr17:1643670
43	SUPV3L1:chr10:69189317	chr10	69189317	69189317	C	T	p.P208L	Missense_Mutation	nonsilent	SNV	SUPV3L1:chr10:69189317
44	FAN1:chr15:30905493	chr15	30905493	30905493	C	G	p.S277C	Missense_Mutation	nonsilent	SNV	FAN1:chr15:30905493
45	TBC1D32:chr6:121131690	chr6	1.21E+08	1.21E+08	C	G	p.E987Q	Missense_Mutation	nonsilent	SNV	TBC1D32:chr6:121131690
46	GLB1L3:chr11:134277852	chr11	1.34E+08	1.34E+08	G	A	p.R101K	Missense_Mutation	nonsilent	SNV	GLB1L3:chr11:134277852
47	CST11:chr20:23452691	chr20	23452691	23452691	C	G	p.E41Q	Missense_Mutation	nonsilent	SNV	CST11:chr20:23452691
48	ZSWIM1:chr20:45884033	chr20	45884033	45884033	G	C	p.E481Q	Missense_Mutation	nonsilent	SNV	ZSWIM1:chr20:45884033
49	RBBP8NL:chr20:62414348	chr20	62414348	62414348	C	G	p.E335Q	Missense_Mutation	nonsilent	SNV	RBBP8NL:chr20:62414348
50	BRAF:chr7:140781611	chr7	1.41E+08	1.41E+08	C	T	p.G466E	Missense_Mutation	nonsilent	SNV	BRAF:chr7:140781611
51	IFT80:chr3:160319905	chr3	1.6E+08	1.6E+08	C	T	p.S271N	Missense_Mutation	nonsilent	SNV	IFT80:chr3:160319905
52	MUC16:chr19:8937521	chr19	8937521	8937521	G	T	p.S11145*	Nonsense_Mutation	null	SNV	MUC16:chr19:8937521
53	PLCE1:chr10:94313273	chr10	94313273	94313273	G	C	p.R2008T	Missense_Mutation	nonsilent	SNV	PLCE1:chr10:94313273
54	ARPC4:chr3:9803843	chr3	9803843	9803843	G	A	p.G111R	Splice_Site	null	SNV	ARPC4:chr3:9803843
55	LRP1:chr12:57192941	chr12	57192941	57192941	G	A	p.R2509Q	Missense_Mutation	nonsilent	SNV	LRP1:chr12:57192941
56	OGG1:chr3:9751889	chr3	9751889	9751889	C	T	p.R169W	Missense_Mutation	nonsilent	SNV	OGG1:chr3:9751889
57	PRKD3:chr2:37316467	chr2	37316467	37316467	G	C	p.P20A	Missense_Mutation	nonsilent	SNV	PRKD3:chr2:37316467
58	PRKD3:chr2:37316242	chr2	37316242	37316242	G	C	p.Q95E	Missense_Mutation	nonsilent	SNV	PRKD3:chr2:37316242
59	PLEKHM1:chr17:45458393	chr17	45458393	45458393	C	A	p.R452L	Missense_Mutation	nonsilent	SNV	PLEKHM1:chr17:45458393
60	RCC1:chr1:28532243	chr1	28532243	28532243	C	T	p.P112S	Missense_Mutation	nonsilent	SNV	RCC1:chr1:28532243
61	NELL2:chr12:44779966	chr12	44779966	44779966	G	A	p.S131L	Missense_Mutation	nonsilent	SNV	NELL2:chr12:44779966
62	DYRK4:chr12:4604947	chr12	4604947	4604947	C	T	p.S272F	Missense_Mutation	nonsilent	SNV	DYRK4:chr12:4604947
63	ATP2B1:chr12:89655717	chr12	89655717	89655717	T	C	p.Y57C	Missense_Mutation	nonsilent	SNV	ATP2B1:chr12:89655717
64	KIF2B:chr17:53823520	chr17	53823520	53823520	C	T	p.R163C	Missense_Mutation	nonsilent	SNV	KIF2B:chr17:53823520
65	ADGRL3:chr4:62063565	chr4	62063565	62063565	C	A	p.P1292H	Missense_Mutation	nonsilent	SNV	ADGRL3:chr4:62063565
66	ZFYVE9:chr1:52266657	chr1	52266657	52266657	C	G	p.Q761E	Missense_Mutation	nonsilent	SNV	ZFYVE9:chr1:52266657
67	TRIM62:chr1:33147393	chr1	33147393	33147393	C	T	p.W283*	Nonsense_Mutation	null	SNV	TRIM62:chr1:33147393
68	TMPRSS11B:chr4:68234565	chr4	68234565	68234565	C	T	p.E123K	Missense_Mutation	nonsilent	SNV	TMPRSS11B:chr4:68234565
69	TIGD7:chr16:3299119	chr16	3299119	3299119	C	G	p.R499T	Missense_Mutation	nonsilent	SNV	TIGD7:chr16:3299119
70	DLX4:chr17:49973080	chr17	49973080	49973080	G	C	p.E97D	Missense_Mutation	nonsilent	SNV	DLX4:chr17:49973080
71	CCDC17:chr1:45623902	chr1	45623902	45623902	G	A	p.S3F	Missense_Mutation	nonsilent	SNV	CCDC17:chr1:45623902
72	CLUH:chr17:2703463	chr17	2703463	2703463	C	G	p.E72D	Missense_Mutation	nonsilent	SNV	CLUH:chr17:2703463
73	HS3ST6:chr16:1911844	chr16	1911844	1911844	C	A	p.E259*	Nonsense_Mutation	null	SNV	HS3ST6:chr16:1911844
74	ANHX:chr12:133231629	chr12	1.33E+08	1.33E+08	C	T	p.G89R	Missense_Mutation	nonsilent	SNV	ANHX:chr12:133231629
75	ATP8B3:chr19:1800082	chr19	1800082	1800082	C	T	p.V473M	Missense_Mutation	nonsilent	SNV	ATP8B3:chr19:1800082
76	CYP2C19:chr10:94842987	chr10	94842987	94842987	C	T	p.T371I	Missense_Mutation	nonsilent	SNV	CYP2C19:chr10:94842987
77	MFAP1:chr15:43812994	chr15	43812994	43812994	G	C	p.R294G	Missense_Mutation	nonsilent	SNV	MFAP1:chr15:43812994

Table S8. List of mutations in Map24 and Map19 (α and β clusters) validated by PCR-based Sanger sequencing, related to Figure 7

Cluster	Gene	Mutation	Mutation call	Sequencing results	Primers	Protein Change	Variant Classification	Effect
Map24 α	PLCB3	PLCB3:chr11:64267452	G to A	G to A	F-CCTGTGATGCCCATCCTTCTC R-AAGCATTAGTGTCATTGCCTCCTG	p.D1201N	Missense Mutation	nonsilent
Map24 α	PACS1	PACS1:chr11:66070590	A to C	A to C	F-GGAAGCCTGGGAGCCAGATC R-ATGGAGGTGGAGGTAGACGAGGAC	p.Q35P	Missense Mutation	nonsilent
Map24 α	OTOP1	OTOP1:chr4:4197744	C to T	C to T	F-ATGGAGTAGGGCAGGTTGTACCAG R-CATTGCTGTGGTGGTGGTATACC	p.A364T	Missense Mutation	nonsilent
Map24 β	CDKN1A	CDKN1A:chr6:36684429	A insertion	A insertion	F-ACTTTGTCACCGAGACACCACTG R-TCCTGGTCCCTTACAAAGTCCTTC	p.H110fs	Frame Shift Ins	null
Map24 β	APC	APC:chr5:112839465	C to T	C to T	F-GCTCCATCCAAGTTCTGCACAGAg R-CAGTCTGCTGGATTTGGTTCTAGG	p.Q1291*	Nonsense Mutation	null
Map24 β	FBXW7	FBXW7:chr4:152337818	G to C	G to C	F-TGGCAATTTATCAATTTACAGCCCTC R-TTTGATAGAGCTGGAGTGGACCAG	p.S202*	Nonsense Mutation	null
Map24 β	BRAF	BRAF:chr7:140781611	C to T	C to T	F-ATGCGAACAGTGAATATTTCCTTTG R-CTGTATCCCTCTCAGGCATAAGG	p.G466E	Missense Mutation	nonsilent
Map24 β	RCC1	RCC1:chr1:28532243	C to T	C to T	F-GAAATGGAGCTGGCTAGTCAAGTG R-CAGACTTTCAGACCCAGCCTTACC	p.P112S	Missense Mutation	nonsilent
Map19 α	ZMIZ1	ZMIZ1:chr10:79292307	T to A	T to A	F-TGCAGGCAGTACCTAACTCTTCCA R-CCATAAGCACTGACATCCCAACTC	p.V303E	Missense Mutation	nonsilent
Map19 α	ERCC2	ERCC2:chr19:45364429	C to G	C to G	F-GTTTTCTCTACCTCTGGGCTAAGG R-TTCGGGGGTGTTTGGGAAGCTG	p.N238S	Missense Mutation	nonsilent
Map19 β	KDM6A	KDM6A:chrX:45063557	C to T	only T	F-AGATGAGACCAACAGGAGTTGCAC R-GCACGTTTCCATTACTTCCACTTCC	p.Q555*	Nonsense Mutation	null
Map19 β	FBXW7-2	FBXW7:chr4:152352482	C to T	C to T	F-AGAATACCAGACATCCAGCCACC R-CCGGTTCTGCTCCCTAATCTTCC	p.M83I	Missense Mutation	nonsilent
Map19 β	CDKN2A	CDKN2A:chr9:21971210	T to A	T to A	F-ACCAGCGTGTCCAGGAAGC R-GGAAACTGGAAGCAAATGTAGGGG	NA	Splice Site	null
Map19 β	KMT2C	KMT2C:chr7:152167145	C to T	C to T	F-GGTCTCAGAGCTGTCACTTTTTGG R-TGAAGAACAAATTGGTGCTCACAG	NA	Splice Site	null
Map19 β	SMARCA4	SMARCA4:chr19:10984249	G to A	G to A	F-CAGACTGACCAGGACTGTCTTCC R-ATCCCTACCTTGTGCATCTGGTG	p.G33D	Missense Mutation	nonsilent
Founder mutations								
Map24 β	BAP1	BAP1:chr3:52403766	G to C	G to C	F-CTGCTAGTCTTGATGGACAGAGGAATT R-CCCTTGCTTCACATCTTCTCG	p.S460*	Nonsense Mutation	null
Map19 β	CAPRIN1	CAPRIN1:chr11:34089401	C to G	C to G	F-GTTTTGGTCACCTTTGCAGTTCATT R-AGTGATCCTCCCATCTCAGC B-TTGCAGTTCATTCTGAATCTAGACTTGCTCAAAAA	p.S413C	Missense Mutation	nonsilent

F-forward primer; R-reverse primer; B-blocking primer